Underwater Ambient Noise at a Proposed Tidal Energy Site in Puget Sound

Christopher Bassett

A thesis submitted in partial fulfillment
of the requirements for the degree of

Master of Science in Mechanical Engineering

University of Washington

2010

Program Authorized to Offer Degree: Mechanical Engineering

University of Washington
Graduate School

This is to certify that I have examined this copy of a master's thesis by

Christopher Bassett

and have found that it is complete and satisfactory in all respects,
and that any and all revisions required by the final
examining committee have been made.

Committee Members:

Jim Thomson

Brian Polagye

Peter Dahl

Date:

Signature____________________________

Date________________________________

University of Washington

Abstract

Underwater Ambient Noise at a Proposed Tidal Energy Site in Puget Sound

Christopher Bassett

Chair of the Supervisory Committee:
Assistant Professor Jim Thomson
Civil and Environmental Engineering

Ambient underwater acoustics data are presented for one-year at a potential tidal energy site in Admiralty Inlet, Washington, USA with maximum currents exceeding 3 m/s. The site, at a depth of approximately 60 meters, is located near shipping lanes, a local ferry route, and a transit area for many cetacean species. A key finding is that non-propagating turbulent pressure fluctuations, termed *pseudosound*, can mask ambient noise, especially in highly energetic environments suitable for tidal energy development. A statistical method identifies periods during which changes in the mode and standard deviation of the one-third octave band sound pressure levels are statistically significant and thus suggestive of pseudosound contamination. For each deployment, recordings with depth averaged tidal currents greater than 1 m/s are found to be contaminated, and only recordings with currents below this threshold are used in the subsequent ambient noise analysis. Mean total sound pressure levels (0.16 - 30 kHz) over all recordings are 117 dB re 1μPa.

Commercial shipping and ferry vessel traffic are found to be the most significant contributor to ambient noise levels at the site, with secondary contributions from rain, wind, and marine mammal vocalizations. Post-processed data from an AIS (Automatic Identification System) receiver is used to determine the location of ships during each recording. Referencing 368 individual recordings with the distance between the ferry and the site obtained from AIS data, the source level of the ferry is estimated to be 179 $\pm$ 4 dB re 1μPa at 1m with a logarithmic spreading loss coefficient of 18.

TABLE OF CONTENTS

LIST OF FIGURES

LIST OF TABLES

GLOSSARY

ADCP: Acoustic Doppler Current Profiler

AIS: Automatic Identification System (used for real-time ship traffic information)

c: Speed of sound (approximately 1500 m/s in seawater)

CPDF: Cumulative probability distribution function

dB: Decibel (log scale)

DOE: Department of Energy

FFT: Fast Fourier Transform

f_o: Center frequency for one-third octave bands

f_n: Nyquist frequency

f_s: Sampling frequency

GB: Gigabyte

Hz: Hz

n: Specific sample within a time series or data set

N: Number of data points in a sample

NMFS: National Marine Fisheries Service

NOAA: National Oceanic and Atmospheric Administration

p: Pressure

p_{ref}: Reference pressure

PDF: Probability density function

Pa: Pascal

PSD: Pressure spectral density

RMS: Root Mean Squared

SPL: Sound pressure level

SRKW: Southern Resident killer whale

TOB: One-third octave band

μPa: Micropascal (10^{-6} Pa)

ACKNOWLEDGMENTS

I would like to express gratitude to Dr. Jim Thomson, Dr. Brian Polayge, and Dr. Peter Dahl for their support and ideas throughout this project. Snohomish Public Utility District made my involvement in this project a possibility by providing financial support and for this I cannot thank them enough. Joe Talbert, thanks for engineering solutions for field deployments. Thanks to Dr. Dominic Tollit of the Sea Mammal Research Unit and Dr. Scott Veirs of Beam Reach Marine Science and Sustainability School for their communications and support in identifying marine mammal vocalizations. I would also like to thank my parents and grandparents, all of whom are a constant source of inspiration. Finally, I would also like to thank Dana Geller, my high school calculus teacher, for making math exciting. Without her calculus class I would not have studied engineering.

Chapter 1

INTRODUCTION

Recent concerns about global climate change and fossil fuel consumption have driven a number of states to adopt binding Renewable Energy Portfolio Standards. Such standards coupled with the growing demand for electricity have led the Snohomish Public Utility District to explore renewable energy sources. Tidal energy, the extraction of energy from tidally driven currents, is one such potential energy source that is being explored. Snohomish PUD has proposed a tidal energy pilot project in Admiralty Inlet.

One of the primary concerns with respect to tidal energy development is the potential impact on the underwater acoustic environment. Marine mammals vocalize and echolocate for social purposes and to hunt for prey. Increased ambient noise levels during installation or normal operation could impede these necessary activities by masking auditory returns. Sound exposure can also lead to avoidance behavior, temporary threshold shifting, and temporary or permanent hearing loss (Holt, 2008). In the case of the proposed tidal energy pilot project, the general concern about the impacts of anthropogenic noise on marine species is exacerbated by the location of the proposed site - it is in a region containing three zones designated as critical habitat areas for Southern Resident killer whales (*Orcinus orca*) (NMFS, 2006). Presently, little is known about the impact of tidal turbines on underwater ambient noise. This research includes a one-year baseline ambient noise study of the proposed pilot project site, analyzes the impact of common ambient noise sources, and prepares a baseline for assessing the impact of any tidal energy development that occurs.

1.1 Site Description

The proposed location of the tidal energy pilot project is Eastern Admiralty Inlet, just west of Admiralty Head at Fort Casey State Park in Washington state. Admiralty Inlet is the primary inlet to the Puget Sound from the Strait of San Juan de Fuca. As a result, the five kilometer wide inlet experiences tidal currents in excess of 3 m/s. The survey area for the tidal project is a 1.5 km x 1.0 km rectangle that is roughly aligned with the principal axis of the flow in and out of the inlet. The bathymetry in Admiralty Inlet is complicated but the site under consideration is relatively flat and approximately 65 m deep. Puget Sound, Admiralty Inlet, and the location of the survey area are shown in Figure 1.1.

Figure 1.1: Puget Sound, Admiralty Inlet, and the survey area represented by the rectangle on the easy side of Admiralty Inlet (right).

1.2 Acoustics Measurements

Pressure levels associated with acoustic measurements cover many orders of magnitude. As a result, it is common convention to report acoustic measurements in units of decibels. Decibels are a unit that require an arbitrary reference value. Accepted convention is to use

1 μPa as the reference pressure in water; this is compared to 20 μPa used as the reference pressure in air. Following convention, throughout this document values will be reported in decibels with a respect to 1 μPa but values will simply be referred to as decibels. Sound pressure levels (SPL) and pressure spectral densities (PSD) will be used throughout the this report and require clarification.

Sound pressure level is defined as the ratio of the RMS pressure squared to the square of the reference pressure. In decibels, the sound pressure level is expressed by Equation 1.1.

$$SPL\ (dB) \ = \ 10\ log_{10}\left(\frac{p_{rms}^2}{p_{ref}^2}\right) \ = \ 20\ log_{10}\left(\frac{p_{rms}}{p_{ref}}\right) \tag{1.1}$$

A curve of the pressure spectral density (PSD) is created by processing the raw data from the hydrophone. The PSD is a measure of the acoustic energy contained in a given frequency band. A more rigorous explanation of signal processing and the definition of pressure spectral density is included in Chapter 2. For underwater sound the resulting units for PSD are dB with respect to one micropascal-squared per hertz (dB re 1μPa^2/Hz). To obtain the sound pressure level associated with a given frequency range, the pressure spectral density can be integrated over the frequency band of interest (Equation 1.2). Integration under the entire curve yields the total sound pressure level associated with the acoustic measurements.

$$SPL\ (dB) \ = \ 10log_{10}\left(\int_{f_1}^{f_2}\ PSD\ df\right) \tag{1.2}$$

The sound pressure attenuation characteristics of seawater have a direct impact on what spectral levels are recorded. Relaxation is the chemical or molecular response to pressure changes associated with sound waves. Both molecular relaxation due to viscosity and chemical relaxation absorb energy contained in sound waves causing the waves to attenuate. Relaxation has a greater effect on high frequency noise resulting in higher attenuation rates. Attenuation rates, measured in dB/km, are approximately four orders of magnitudes larger for 10 kHz sounds than they are for 100 Hz sounds. As a result, low frequency sounds from sources such as shipping vessel can propagate thousands of kilometers in the open ocean while high frequency sounds are rapidly attenuated (Medwin, 2005).

1.3 Ambient Noise

Ambient noise is often defined as the noise at a site in the absence of anthropogenic noise sources. For this study, as a result of the regularity of marine traffic at the proposed site, ambient noise will be discussed as the noise at the site without regard to the presence of anthropogenic noise in order to characterize typical conditions. By this definition, underwater ambient noise can be attributed to three unique categories of sources: natural physical processes, biological sources, and anthropogenic sources. Within each category of sources, a variety of mechanisms produce the sound over different frequency ranges. Past research has identified ambient noise sources and the spectral levels and frequencies at which common sources impact the acoustic environment. Ambient noise sources at low frequencies that affect sound levels in this study include ship traffic ranging from shipping vessels, recreational boats, and ferry traffic. Oceanic traffic influences spectral levels from 10 Hz to beyond 10 kHz with the dominant components occurring at low frequencies. Wind speed is shown to be the dominant source of sound between 100 Hz and 10 kHz in the absence of anthropogenic sources. Bubbles and spray are attributed to surface agitation affect the spectral levels from 100 Hz to as high as 30 kHz. Contributions from rainfall are also associated with surface agitation and spray. At frequencies above 10 kHz thermal noise associated with molecular agitation occur at decibel levels that increase with frequency (Wenz, 1962; Mellen, 1952). The following paragraphs introduce the mechanisms of sound production for these important underwater sources in greater detail.

A broad range of natural processes affect the underwater acoustic environment over a broad range of frequencies. Earthquakes, microseisms, second-order effects from surface waves, and oceanic turbulence cause pressure fluctuations that can be measured by hydrophones. Although the low frequencies at which some of these sources contribute to ambient noise spectra are not considered in this research, a description of their contributions has been included for completeness. Microseisms occur at frequencies less than 1 Hz (Urick, 1967). Regular seismic activities like earthquakes can affect acoustic spectra up to 100 Hz but are intermittent sources (Wenz, 1962). Second order surface waves effects contribute to acoustic spectra at frequencies between 0.1 Hz and 5 Hz (Medwin, 2005). First order effects of wind driven surface waves create pressure fluctuations in the water column but are not important for ambient noise measurements in bottom mounted hydrophones because the pressure fluctuations attenuate exponentially with depth and because the frequency range over which they occur is not covered by this study (Urick, 1967).

Turbulent pressure fluctuations can impact acoustic measurements by two different mechanisms. The first mechanism is the measurements of oceanic turbulence. Pressure fluctuations associated with turbulent flow advected over a hydrophone have been measured in environmental flows. One example of field work demonstrating this impact is from Narragansett Bay, Rhode Island. There, hydrophone measurements in the one-third octave band centered at 25 Hz were shown to increase during periods of strong tidal currents (Willis and Dietz, 1965). Although turbulent pressure fluctuations are measured by hydrophones, they are not propagating sound and are therefore referred to as "pseudosound." There is also a small radiated component of noise produced by turbulence. The impacts of the propagating noise from turbulence are minimal because they radiate at a low efficiencies and decay rapidly with distance (Urick, 1967).

Another contributor of pseudosound is interactions between the turbulent pressure field and the hydrophone. It has been shown that pressure fluctuations in the hydrophone boundary layer are greater in magnitude than pressure fluctuations of the turbulent field alone and that the impacts of boundary layer fluctuations are greatest at low frequencies and dependent on hydrophone geometry (Strasberg, 1979). Attempts to describe wind screen noise on microphones using non-dimensional parameters have been successful but similar non-dimensionalization of hydrophone flow-noise were less successful. Some suggestions for the this include differences in the construction of hydrophones as well as susceptibility of hydrophones to vibrations caused by swift underwater currents (Strasberg, 1988). One method employed to identify pseudosound is calculating signal coherence, a frequency space measure of the correlation of two independent signals. For propagating sound the coherence between two hydrophones separated by a short distance will be high but the coherence of psuedosound measurements will be low due to the chaotic nature of turbulence. The method requires two hydrophones and has been employed in studies of ambient noise to identify periods of pseudosound (Deane, 2000).

A familiar example of flow noise would be an individual standing outside on a windy day that hears a ruffle in their ear due to the wind. A person standing nearby but protected from the wind would not hear the same ruffling noise because it is not a result of a propagating sound wave. Regardless of the underlying physics of pseudosound, acoustic spectra that are contaminated by pseudosound are not propagating ambient noise and should not be included in descriptions of the underwater acoustic environment.

The contribution of wind speed to ambient noise is a result of breaking waves at the air-sea interface caused by wind stress. The breaking waves entrain acoustically active bubbles which produce sound at frequencies dependent on the bubble diameter (Ma et al., 2005). Wind generated sound has a constant negative spectral slope that is independent of wind speed between 500 Hz to 50 kHz independent of wind speed (Ma et al., 2005; Medwin, 2005). Although sea state is a commonly used describe surface conditions, the correlation between the wind speed and underwater noise levels is stronger than that between sea state and noise levels (Wille and Geyer, 1984). Due to the proximity of the proposed site to the shore, surf noise may also impact ambient noise spectra. Surf noise generates noise between 100 Hz and 20 kHz at the interval of waves breaking on the shore (Deane, 2000).

The effects of rainfall rates on acoustic spectra are dependent on droplet sizes and wind speed. Typical precipitation rates in the study area typically fall under the category of "light" (< 2.5 mm/hr) and occasionally "moderate" ($2.5 > R < 7.5$ mm/hr) rainfall rates. Small droplets associated with light rainfall produce sound through two mechanism: the droplet impact creates broadband noise which is followed by louder resonating microbubble. The resonant frequency of these entrained microbubbles ranges from 12 to 21 kHz with an average of 15 kHz (Medwin et al., 1992). Noise from precipitation during light rainfall events is highly dependent on wind speed. The likelihood of bubble creation by an individual droplet is 100% at a normal incidence angle but decreases to 20% for incidence angles of

20° (Ma et al., 2005). Increased wind speeds during periods of light rain decreases peak spectral levels, widens the peak, and increases the peak frequency (Nystuen and Farmer, 1987). During periods of moderate precipitation rates the contribution of the rain to ambient noise is primarily a result of the intial droplet impact on the surface (Medwin et al., 1992). Acoustic spectra during moderate rain conditions decrease linearly between 1 to 15 kHz before rolling off around 15 kHz (Ma et al., 2005).

At very high frequencies thermal noise determines the limit of effective acoustic measurements. If all other noise sources were removed, the resulting measurements would be attributable to the thermal excitation of water molecules (Mellen, 1952). At the frequencies under consideration in this study, ambient noise exceeds the thermal noise limits.

Sources of anthropogenic noise in marine environments include pile driving, air guns arrays, ship traffic, and industrial activity. With the exception of ship traffic, anthropogenic noise sources are not considered in this research but a discussion of their characteristics has been included for completeness. Peak source levels attributed to pile driving can reach 210 dB re 1 μPa at a 10 m range with peak frequencies under 1 kHz (Dahl, 2010). Air guns arrays used in seismic exploration, commonly used in the energy industry to search for fossil fuel deposits, have sources levels of up to 256 dB re 1 μPa at 1 m with a peak frequency between 5 Hz and 300 Hz (Hildebrand, 2004). The impacts of industrial activity on ambient noise are typically at tones related to the rotational frequencies of turbomachinery (NRC, 2003).

Ambient noise measurements taken over many decades in the open ocean and in coastal environments show a long term trend of increasing ambient noise levels except in the South Pacific and South Indian Ocean where there is little shipping traffic (Ross, 1976). These increases are result of increased anthropogenic noise, particularly ship traffic. The primary sound of low-frequency ambient noise in areas with high shipping densities is ship traffic (Dahl et al., 2007). Explanations for the sustained increases in ambient noise levels include increases in ship traffic, engine power, ship speed, and gross tonnage carried by merchant vessels (Hildebrand, 2005; Ross, 1976).

The most common source of anthropogenic noise in Admiralty Inlet is ship traffic. Ship traffic, regardless of size, produces sound by mechanical noise, flow over the hull, cavitation due to the propeller, and through the use of various active acoustic technologies (e.g. depthsounders). Military and commercial sonars have a wide range of applications and associated frequencies. Peak frequencies range from low ($<$ 1 kHz) to very high ($>$ 200 kHz); source levels across the peak frequency range for different sonars reach 235 dB (Hildebrand, 2005). Cavitation due to a pressure drop across the propeller creates broadband noise. Low frequency tonal contributions to the ambient noise spectra are related by multiples of the number propeller blades multiplied by the revolutions per second (Arveson and Vendittis, 2000). Mechanical noise and its impact on ambient noise can be traced to the firing rate of the onboard diesel engines, gearing, pumps and other mechanical equipment. Hydrodynamic flow over the hull of the ship can also contribute to broadband radiated noise, particularly at high velocities (Hildebrand, 2005).

Source levels for ship traffic vary significantly based on the size and speed of the vessel. Every ship has a unique acoustic signature which relates to ship speed, the condition of the vessel, vessel load, and on-board activities (Ross, 1976). Source levels for ship traffic range from 150 dB for small fishing vessels to 195 dB for super tankers (Gray and Greeley, 1980; Hildebrand, 2005). Peaks in spectral levels for shipping traffic occur at less than 500 Hz with substantial tonal contributions below 10 Hz (Scrimger and Heirmeyer, 1991). Studies on small ship traffic show peak spectral levels of 145 dB re $1\mu\text{Pa}^2/\text{Hz}$ between 350 to 1200 Hz (Hildebrand, 2005).

Marine mammal vocalizations and echolocations are the primary sources of potential biological noise. Marine mammals that are found in the Puget Sound include, but are not limited to, killer whales, harbor porpoises, Dall's porpoises, gray whales, minke whales, harbor seals, California sea lions, Stellar sea lions, and elephant seals (Shepard, 2009). Marine mammal vocalizations occur over a wide range of frequencies. For example, dominant frequencies for gray whales are as low as 20 Hz and harbor porpoise echolocation clicks exceed 100 kHz (Whitlow et al., 2000). Frequency ranges associated with orca and harbor porpoise vocalizations are included in Table 1.1.

The most concern and interest with respect to the impacts of tidal energy on ambient noise is directed at the Southern Resident killer whale (SRKW). Southern Resident killer whales differ from transient orca populations in that their diets consist of primarily of fish rather than other marine mammals, they live in stable pods, and have smaller ranges (NMFS, 2008). The SRKW population inhabits the inland waters of the Salish Sea from late spring to early fall (Holt, 2008). The SRKW populations occasionally transit Admiralty Inlet to enter the Puget Sound; most SRKW sitings in the Puget Sound occur between October and January (Whale Museum, 2009).

Communications used by killer whales can be broken into vocalizations (whistles and pulsed calls) and echolocations. Whistles are used for social communication (Richardson et al., 1995). Pulsed calls are used when foraging and traveling to maintain social cohesion (Ford, 1989). Transient and resident communities have developed unique dialects and vocalization patterns (Ford, 1991). Frequency ranges for whistles and pulsed calls are 1.5 kHz to 18 kHz and 0.5 kHz to 25 kHz respectively. Dominant frequencies for whistles are 6 kHz to 12 kHz and 0.5 kHz to 6 kHz for pulsed calls (Ford, 1989). Field research on foraging resident killer whales shows that most echolocation clicks have a bimodal distribution with a low-frequency peak between 20 and 30 kHz and a high-frequency peak between 40 and 60 kHz. The echolocation clicks have average bandwidths between 35 and 50 kHz (Au et al., 2004). Transient killer whales rarely use echolocation to hunt prey; the use of echolocation amongst residents while foraging is common (Deeke et al., 2005).

Table 1.1: Frequency ranges for common marine mammals in Puget Sound (Richardson et al., 1995)

Species	**Call Type**	**Call Range (kHz)**	**Echolocation Range (kHz)**
Orca	Whistle	1.5-18	12-25
	Pulsed	0.5-25	
Harbor porpoise	-	2	110-150

1.4 Analysis

The ambient noise analysis included in this report cover frequency bands from 20 Hz to 30 kHz; the results are reported for the entire frequency band covered by the data and one-third octave bands. Throughout the report, total sound pressure levels will refer to the frequency range 0.156 - 30 kHz unless otherwise noted. The frequency ranges covered are a result of sampling limitations during the long term deployment of the equipment at the site. Specific sources that are addressed include the rain, ship traffic, and suspected biological noise. Analysis of ship traffic focuses on using Automatic Information System (AIS) data to verify the location of ships in the vicinity of the site. Precipitation can only be verified using data from the Washington State University Agricultural Weather Network (AgWeatherNet) station located 3.5 miles north-northeast of the survey area on in Whidbey Island. This data confirms rainfall on an hourly and daily basis at the site of the meteorological station. Rainfall analysis is based on searching for the acoustic signature of light precipitation in the acoustic spectra. Lastly, suspected biological noise analysis is based on reports of marine mammals in Admiralty Inlet by Orca Network and vocalization autodetections from the Port Townsend hydrophone operated by the Port Townsend Marine Science Center.

Chapter 2

INSTRUMENTATION AND METHODOLOGY

The data for acoustic analysis of the site are derived from of two different systems: A recording hydrophone mounted on a tripod that rests on the seabed and a cabled hydrophone deployed from a research vessel. The recording hydrophone remains on the seabed and provides long-term acoustic information about the site. A cabled hydrophone is used during research cruises to obtain spatial acoustic information in real time.

A total of four different sampling configurations were used by the recording and cabled hydrophones throughout the study period. Due to configuration changes, small changes were made to the processing algorithm to optimize bandwidth. The processing steps used are well understood and covered in texts on spectral analysis such as Priestley (1981) and Bracewell (2000). An example of the steps in the processing algorithm is included for two recordings from the November, 2009 to February, 2010 hydrophone deployment. Specific information on sampling configurations, changes to the processing algorithm for individual deployments, and instrument calibration curves is included in their respective sections.

The raw signal is initially broken up into individual windows, or subsets of the raw signal. The window length is chosen to optimize the bandwidth of the final results. For a window with N data points, the final spectrum contains $2/N + 1$ values and is symmetric around the zero frequency (i.e. the mean). Only positive frequencies are valuable in the analysis. The frequency bins associated with the positive frequencies in the spectrum are calculated by evenly spacing the values from the minimum frequency to the Nyquist frequency (f_n), the maximum resolvable frequency which is equal to one-half of the sampling frequency (f_s). For example, during the November, 2009 to February, 2010 deployment the recording hydrophone sampled at 80 kHz. Windows were broken into 4096 data points. The resulting spectra contain 2048 positive frequencies ranging from 19.53 Hz to 40 kHz with a bandwidth of 19.53 Hz. Details about the windows used for other data sets are included in their respective sections.

To calculate the spectra, the mean is first removed from the raw signal of each window. The signal in each series can be expressed as a summation of sine curves with different amplitudes and phases. The transformation from time to frequency space is done using a FFT (Fast Fourier Transform) algorithm. The transformation of a discrete signal into frequency space inevitably leads to leakage. Leakage is the transfer of energy from one frequency bin into another as a result of transformation on the finite time series. The problem of leakage is unavoidable but tapering functions can be applied to each window based on the desired characteristics of the final spectra. For all processing a Hann window is used. A Hann window is a raised cosine function described by Equation 2.1 where n is an integer of the values $0 \leq n \leq N-1$ and N is the number of data points in the window. The Hann window has two desirable effects on the final results. First, by forcing the raw signals to zero at the ends of the window tapering reduces leakage by removing discontinuities in the signal. Second, a Hann window increases the roll-off of the side lobes that result from a transformation into frequency space making it easier to resolve components of the signal with different amplitudes and frequencies. One downside of the Hann windows is that the main lobe of the transform is wider than that of a rectangular, or Boxcar window, making is harder to resolve signals with similar amplitude and frequencies.

$$Hann\ Window \ = \ 0.5 - 0.5\ cos\left(\frac{2\pi n}{N-1}\right) \tag{2.1}$$

Parseval's theorem states that the integral of the pressure spectral density spectrum is equal to the variance of the raw signal. By using a Hann function to taper the original signal the initial variance is altered and a correction factor must be applied to signal to account for the chance in variance. The correction factor for a Hann window is $\sqrt{8/3}$ (Emery and Thomson, 1997). The transformation from time space to frequency space is a linear transformation so the factor can be applied to the spectrum or the tapered time series. In the algorithm used for processing the acoustics data the correction factor was calculated by multiplying the pressure spectral density, in units of pressure, by the factor required to force the variance to match before converting to decibels. An example of a raw signal, a tapered signal, and a tapered signal multiplied by the correction factor for a recording from November 16, 2009 at 16:40.

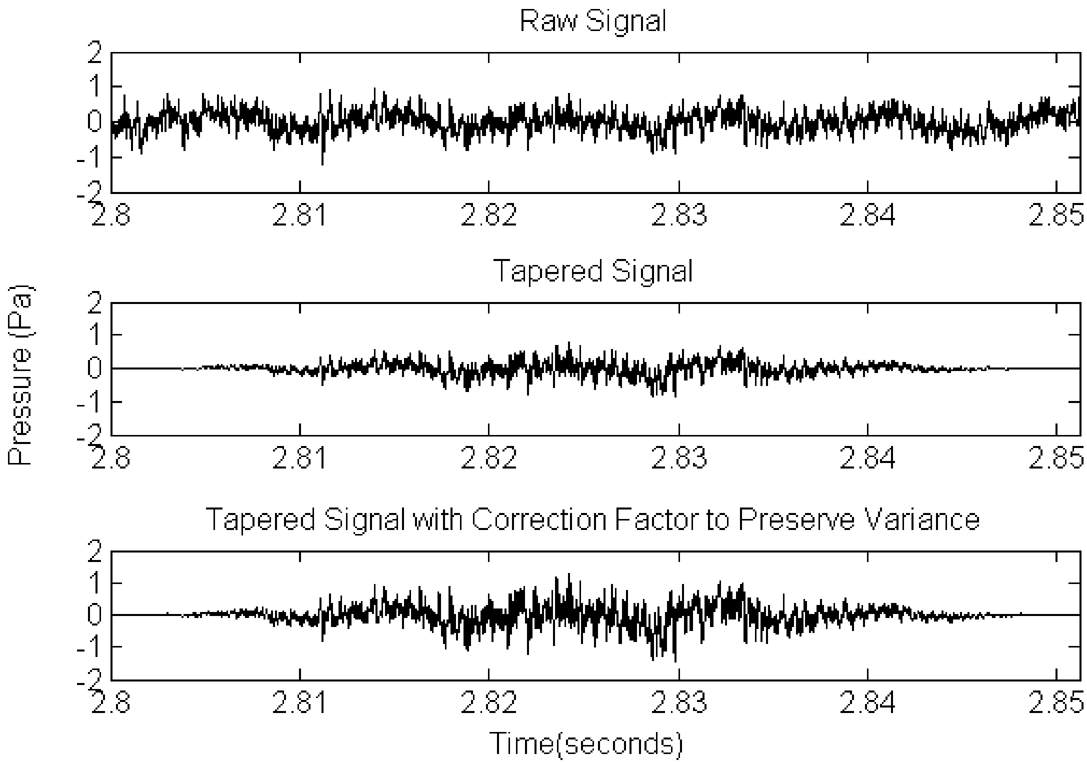

Figure 2.1: Raw signal, tapered signal, and tapered signal with correction factor from 11/16/2009.

The tapered signal is converted to the frequency domain through a Fast Fourier Transform (FFT) algorithm. The pressure spectral density is the modulus squared of the FFT is normalized by the sampling frequency and the number of data points in the raw signal. The value is multiplied by two because only the positive frequencies are used. The pressure spectral density is represented by Equation 2.2. The spectrum, as previously mentioned, is then multiplied by the correction factor needed to satisfy Parseval's theorem.

$$PSD = \frac{1}{f_s N} \left| \sum_{n=1}^{N} x_n e^{-i(2\pi f/f_s)n} \right|^2 = \frac{2\ |FFT|^2}{f_s\ N} \tag{2.2}$$

There is a trade-off between the desired bandwidth (frequency resolution) and the underlying statistics (uncertainty) of the spectrum. Increasing the number of data points per window increases the resolution but decreases the number of spectra which can be ensemble averaged to produce the final spectrum. Besides resulting in a smoother spectrum, each independent window used in the ensemble average represents two degrees of freedom in a chi-squared distribution. The greater number of degrees of freedom used to calculate the spectrum the smaller the uncertainty associated with the spectrum.

Figure 2.2 includes the pressure signal and pressure spectral densities for two recordings from November 16, 2009 demonstrating how the pressure signals and acoustic spectra vary under different acoustic conditions. Larger pressure fluctuations are associated with louder sounds. Shorter oscillation periods of a given magnitude are indicative of higher frequencies. By inspection of the raw signal, it is clear that the sound pressure level in the recordings are much greater at 12:40 than at 16:40. It is also clear that the largest contributions to the sound pressure level at 12:40 are at a low frequencies. These relationships are clearly demonstrated by the resulting spectra. The total SPL during the 12:40 recording is 129 dB and at 16:40 the total SPL is 109 dB.

2.1 Recording Hydrophone

A Loggerhead Instruments DSG long-term acoustic recorder equipped with a High-Tech Inc. hydrophone is mounted on a tripod and deployed at the site. The hydrophone and system frequency response can be seen in Figure 2.3. The sensitivity of the hydrophone is -185.5 dB-V/μPa. A preamplifier applies a 10x voltage gain for an effective sensitivity of -165.5 dB-V/μPa before converting the analog signal to a 16 bit digital signal. The frequency response is approximately flat ($\pm$ 3 dB) from 10 Hz to 30 kHz. The data is logged on a 16 GB SD card which is recovered upon retrieval of the tripod. Other instrumentation on the tripod includes, but is not limited to, an Acoustic Doppler Current Profiler (ADCP), devices (PODS) to detect marine mammal echolocation clicks, and equipment to monitor the temperature, salinity, hydrostatic pressure, and dissolved oxygen. The Loggerhead DSG

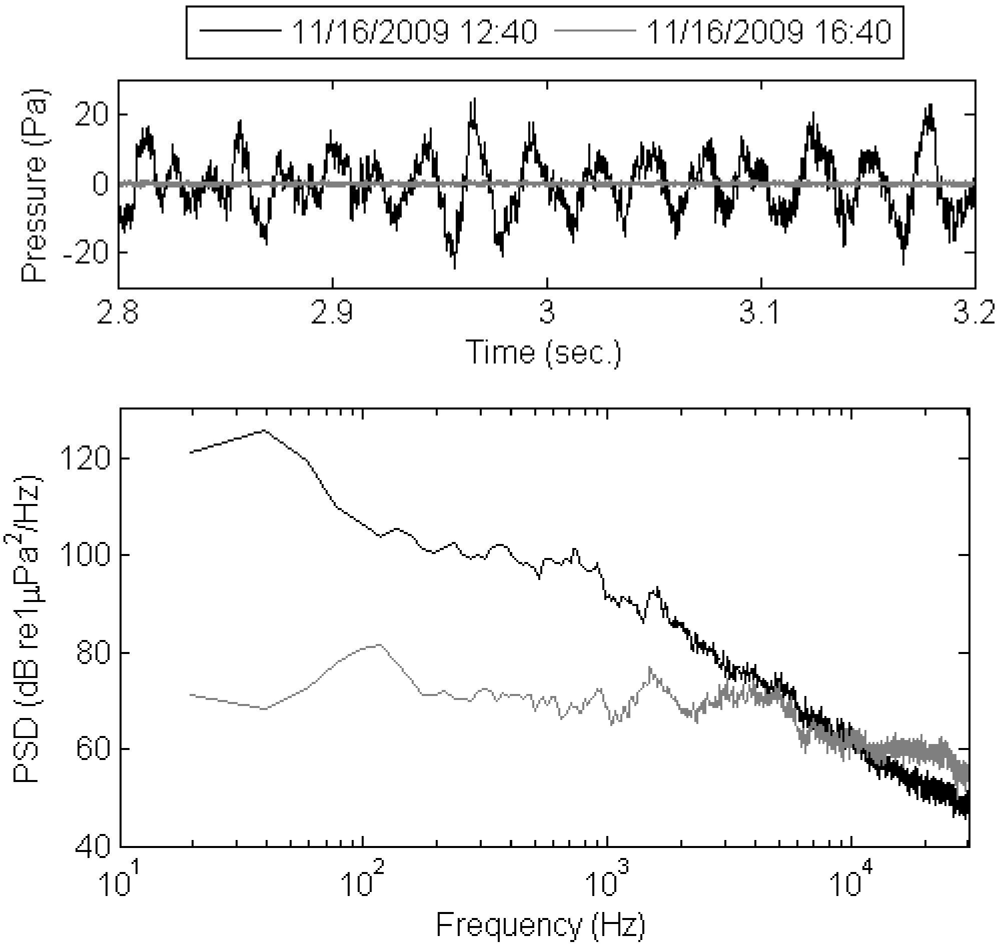

Figure 2.2: Comparison of raw signals and acoustic spectra for two recordings from 11/16/2009.

system is referred to as the recording hydrophone.

The first deployment period for the recording hydrophone began May 19, 2009 and ended on August 3, 2009. The coordinates of the first deployment are 48.1509°N, 122.6878°W. The coordinates of the second deployment, from August 5, 2009 to November 11, 2009 are 48.1491°N, 122.6913°W. During the first two deployments the hydrophone sampled for one minute out of every ten. Within each 60 second sample, the data was staggered to record bursts of 410 out of 4096 data points, a form of data compression that allow acoustic sampling throughout long deployments. A sampling rate of 80 kHz was used in order to

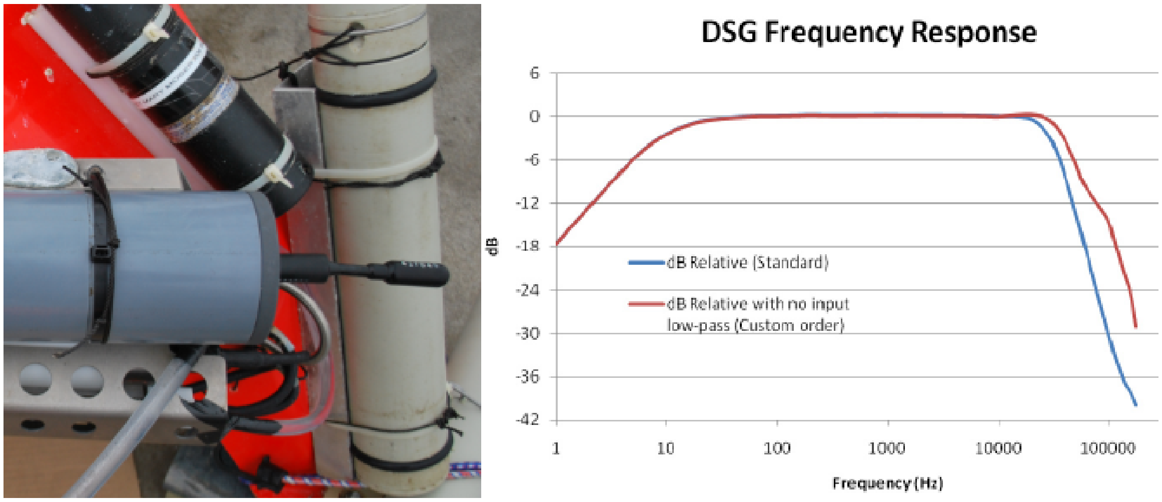

Figure 2.3: Recording hydrophone (grey cylinder with protruding black hydrophone head) prepared for deployment and calibration curve.

permit the resolution of signals up to 40 kHz. The resulting spectra have a bandwidth of 156.25 Hz.

The coordinates of the third deployment, from November 12, 2009 to February 10, 2010 are 48.1477°N, 122.6903°W. The coordinates of the fourth deployment, from February 11, 2010 to May 4, 2010 are 48.1501°N, 122.6862°W. During the third and fourth deployments the sampling was continuous for eight seconds every ten minutes. A sampling rate of 80 kHz was permits the resolution of signals up to 40 kHz. The sampling configuration was changed to improve frequency bandwidth and resolution. Each sample is broken into windows with 4096 data points with a 50% overlap. The resulting acoustic spectra have a bandwidth of 19.53 Hz. The coordinates and survey areas for all of the deployments are shown in Figure 2.4.

2.2 Cabled Hydrophone

Spatial measurements are obtained from a research vessel by a Cetacean™Instruments C54XRS cylindrical omni-directional hydrophone. The Cetacean Instruments™C54XRS has a sensitivity of -185.5 dB-V/μPa and is calibrated for a frequency range of 20 Hz - 250 kHz. The flat frequency response is flat ($\pm$ 3 dB) from 20 Hz to 40 kHz (Figure 2.5). A 10x

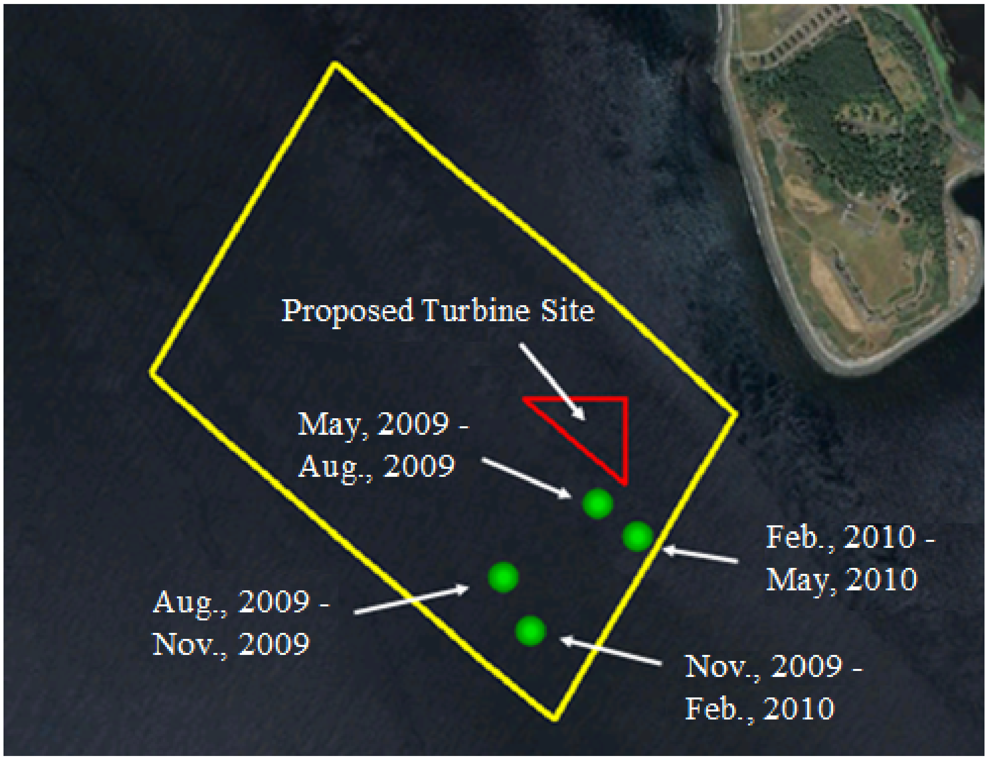

Figure 2.4: The survey area and deployment coordinates for all four deployments.

internal preamplifier produces an effective sensitivity of -165.5 dB-V/μPa. An Iotech DAQ 3001 data acquisition system provides a 1 MHz/16 bit interface that connects to an on-board laptop computer. Each sample carried out with the cabled hydrophone is 60 seconds long with continuous data acquisition. Recordings taken during the first deployment were sampled at a frequency of 200 kHz, permitting the resolution of signals up to 100 kHz. During the second, third and fourth deployments, the system sampled at 400 kHz resulting in resolution of signals up to 200 kHz.

The 50 m mobile hydrophone cable and portable data acquisition system allowed for spatial sampling of the site from the deck of the R/V Jack Robertson. The survey plan included taking samples at the likely deployment site of the tidal turbine as well as a series of concentric circles surrounding the site at a range of 250 m, 500 m, 1000 m, 1500 m, 2000 m, and 2500 m. During the samples the research vessel drifts freely through the concentric circles surrounding the site. At each range, recordings were taken at 3 m, 25 m and 50 m below the surface. All engines, generators, and other sources of noise on-board the ship are disabled during recordings.

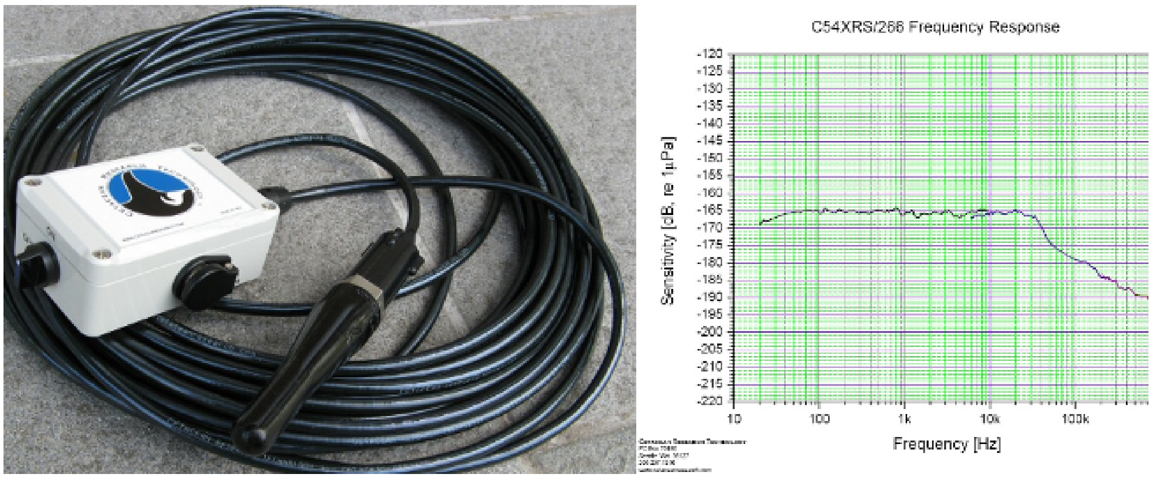

Figure 2.5: Cetacean Instruments hydrophone, deck box, and calibration curve.

A photo of the cabled hydrophone and a plot of the hydrophone's frequency response are included in Figure 2.5. The raw voltage data from each cruise are divided into 180 windows with a 50% overlap. The windows contain 131,072 points for samples during the first cruise. Each window for data from the second, third and fourth cruises contains 262,144 data points. For all cabled hydrophone recordings the resulting bandwidth is 1.526 Hz.

2.3 AIS Data

Automatic Identification System (AIS) is short range marine traffic tracking system. Vessels over 300 tonnes gross weight and passenger vessels are required by the US Coast Guard to carry AIS transceivers, though some smaller vessels do so voluntarily. Vessels equipped with AIS systems transmit signals over very high frequency (VHF) transceivers. The signals are typically used in real time by local ship traffic to avoid collisions. AIS signals include an identification number, ship coordinates, speed over ground, and course of ground every three to ten seconds while the vessel is moving. Additional information such as ship name, ship length, destination, and type of vessel sent every six minutes. In order to verify the presence of ship traffic in ambient noise data in Admiralty Inlet, an AIS receiver installed on the Admiralty Head lighthouse at Fort Casey State Park records the real time data. A coaxial cable runs from the receiver to a data acquisition computer located in basement of the lighthouse. A Python script reads all received AIS data strings through a serial port, writes the AIS strings to file, and includes an epoch time stamp for the received signal. Post processing of the AIS strings are carried out using a Python code written for AIS decoding written by Dr. Kurt Schwehr as part of the University of New Hampshire/NOAA Chart the Future project.

Chapter 3

PSEUDOSOUND

Taking underwater acoustics measurements in highly energetic regions like Admiralty Inlet presents unique challenges for proper interpretation of the data. The impact of psuedosound, produced by turbulent pressure fluctuations during periods of high velocity, is different during each deployment. The problem of pseudosound due to oceanic and boundary layer turbulence is compounded by the wake produced by the tripod, floats and other instruments. These differences are related to both the orientation of the hydrophone and the spatial variability of tidal currents within the survey area. Calculations of coherence to identify periods of flow noise are not possible with only one hydrophone so an indirect method must be used to identify periods of psuedosound. Figure 3.1 shows that the minimum recorded total SPL increases the with increases in depth averaged velocities suggesting that pseudosound is contaminating ambient noise measurements. Figure 3.2 includes spectral pressure densities created by taking ensemble averages of spectra for 0.25 m/s velocity bins during the November, 2009 to February, 2010 deployment. The color of each spectra denotes the depth averaged velocity as shown by the color bar. Negative velocities refer to ebb tide currents and positive velocities refer to flood tide currents.

Spectral levels in the lower frequencies are dominated by loud but distant sources such as ship traffic. Because ship traffic is loud, pseudosound does not mask low frequency propagating noise when it is sufficiently close to the deployment site. Mid-frequencies are dominated by a loud persistent source at approximately 1.5 kHz. Underwater a frequency of 1.5 kHz corresponds to a wavelength of 1 meter, approximately the size of the tripod, suggesting that the vibrations from the sea spider may be the source. Because the noise source is loud and local it is not masked by pseudosound. At high frequencies the sources are relatively quiet and distant sources that are attributed of bubble entrainment at the surface and cavitation from ship propellers. Psuedosound easily masks ambient noise at high frequencies because the sources are weak and remote.

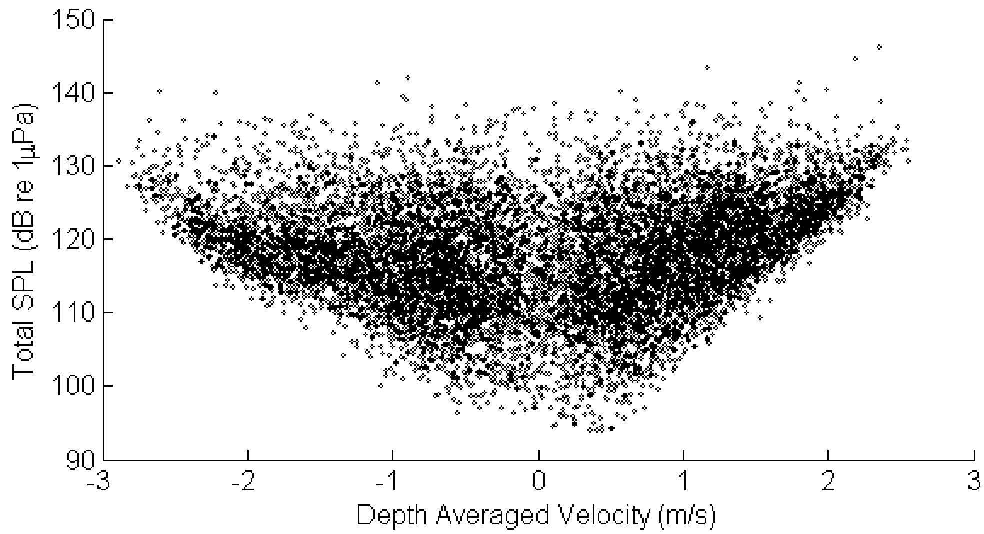

Figure 3.1: Total SPL versus depth averaged velocity for November, 2009 to February, 2010 deployment.

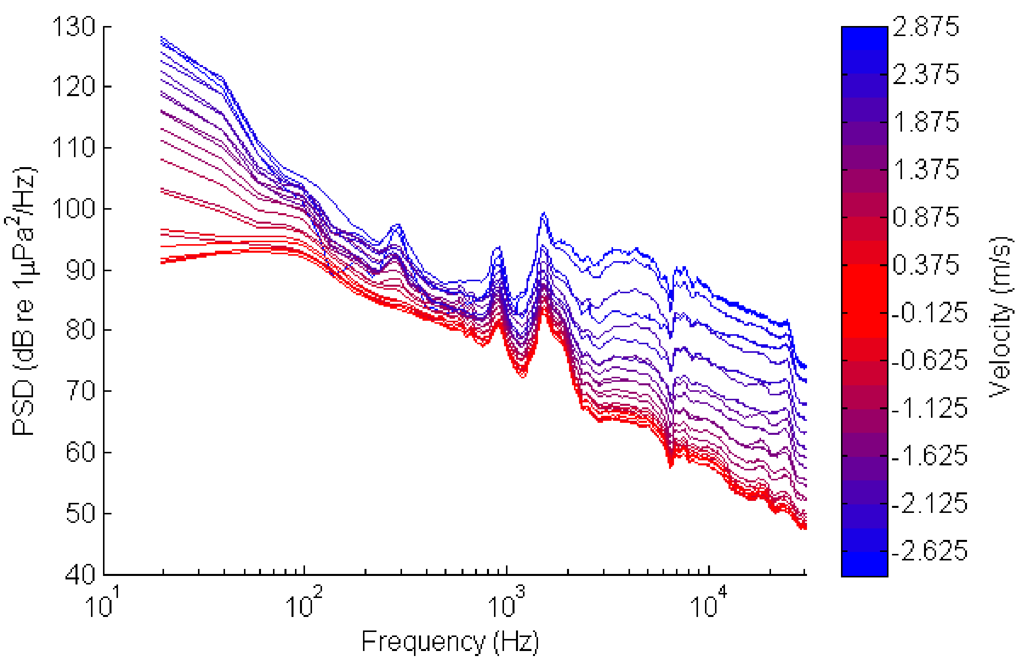

Figure 3.2: Average acoustic spectra for different velocity bins.

Figures 3.1 and 3.2 suggest that recorded total sound pressure levels and pressure spectral densities are not independent of tidal currents at the site and that the increased spectral levels from psuedosound during periods of higher velocity mask ambient noise signals throughout the spectra. Figure 3.3 is a scatter plot of the sound pressure levels in the one-third octave band centered at 2.5 kHz for the November, 2009 through February, 2010 deployment. Around slack tide ($|u| < 0.25$ m/s) the variance of the SPL is greatest and the mean SPL is lowest. As the magnitude of the velocity increases, the variance of the SPL decreases, and the mean SPL increases.

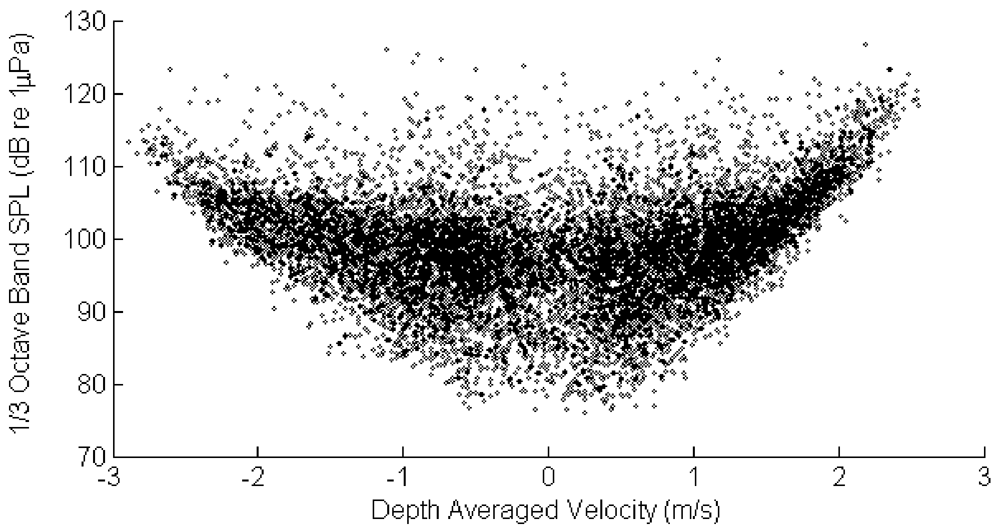

Figure 3.3: SPL in TOB with center frequency of 2.5 kHz versus depth averaged velocity.

The data are analyzed to determine which acoustic recordings are contaminated by pseudosound. Independent analysis of one-third octave band SPLs with velocity bins of 0.25 m/s are used. For a given one-third octave band and velocity bin the SPL distribution is Gaussian suggesting moment analysis is an effective method for eliminating recordings contaminated by pseudosound. Cross sections of the one-third octave band SPL versus depth average velocity scatter plot (Figure 3.3) are used to compare distribution modes and standard deviations across velocity bins for different frequencies. A plot of the probability density function (PDF) of sound pressure levels for the 2.5 kHz, one-third octave band from the November, 2009 to February, 2010 deployment demonstrates that for increasing depth averaged velocities the mean SPL increases while the standard deviation of the SPL decreases (Figure 3.4). Data points are placed on the plot with Gaussian distributions of the same statistics for comparison. The subscripts on the legend refer to the mean depth averaged velocity of the analyzed bins. The clear differences between the distributions of the same frequency but different velocity suggest that acoustic conditions at the higher velocity are unique from those at slack tide.

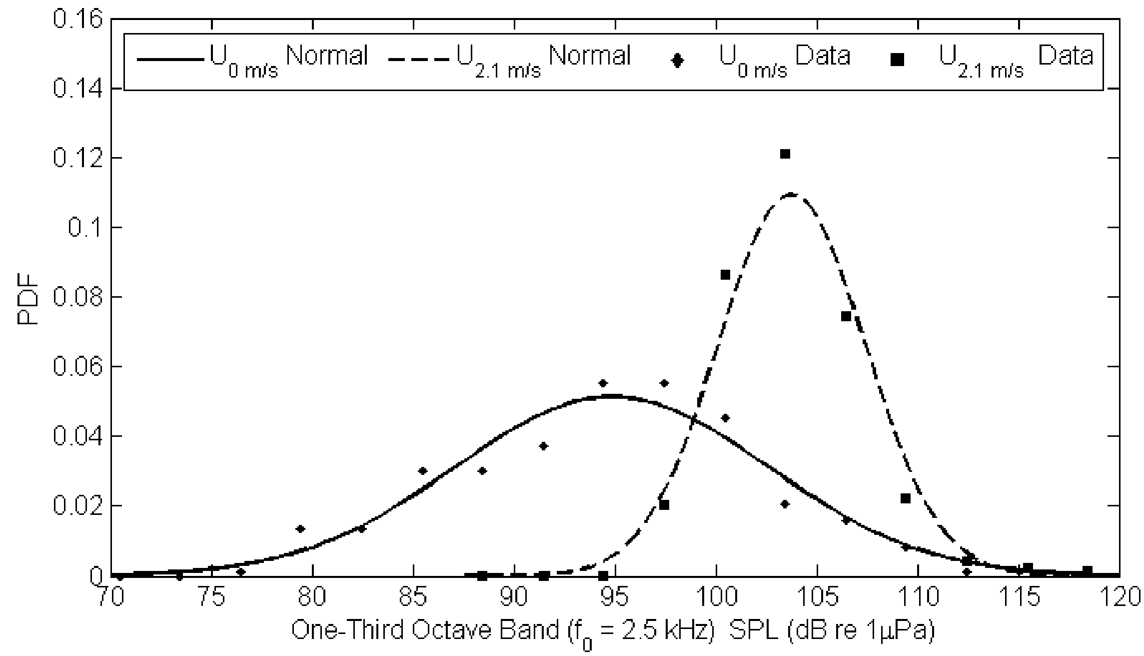

Figure 3.4: TOB SPLs for different velocity bins are normally distributed but have different modes and standard deviations in different velocity bins.

A graphical representation of the statistics used to select uncontaminated data for the November, 2009 to February, 2010 deployment are included in Figure 3.5. The top window shows the shifting modes for each frequency and velocity bin. The slack tide modes and standard deviations are calculated using all recordings in which the depth averaged velocity is between -0.25 to 0.25 m/s. The modes for the slack tide are subtracted from all other velocity bins to show the mode shifting with velocity as represented by Equation 3.1.

The second window is a function of the normalized standard deviation calculated by Equation 3.2. The standard deviation is normalized at each bin by the standard deviation of the slack tide bins at the same frequency. For samples uncontaminated by pseudosound Equation 3.2 is approximately equal to zero. As depth averaged velocity increases, the normalized standard deviation decreases so the results from Equation 3.2 increase. Only velocity bins in which there is no significant shift in mode or normalized standard standard deviation at any frequency are used for ambient noise analysis. Proper one-third octave bands cannot be resolved under 1.25 kHz for the first two deployments so the closest approximations are used.

$$\Delta\overline{SPL} \;=\; \overline{SPL}_{f,v} - \overline{SPL}_{f,0} \tag{3.1}$$

$$1 - \sigma_{normalized} = 1 - \frac{\sigma_{f,v}}{\sigma_{f,0}} \tag{3.2}$$

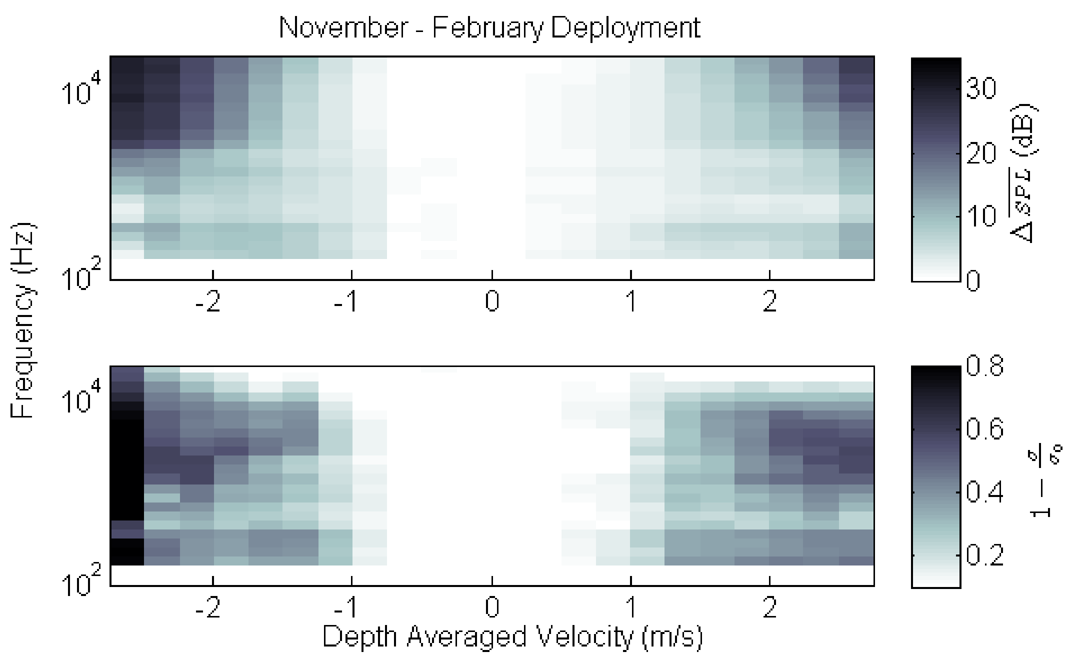

Figure 3.5: Mode shift and normalized σ shift for November to February deployment.

Figure 3.6 includes mode shift and normalized standard deviation shift for all four deployments. While the magnitude of the changes to the modes and standard deviations changes with deployment, the same patterns persist. The total number of samples from each survey and the number retained for ambient noise analysis is shown in Table 3.1. The number of recordings contaminated by flow noise changed for each deployment due to the different orientations and velocity magnitudes but the results of the analysis for flow noise have similar results. For each deployment, recordings taken during periods with depth averaged velocity magnitudes less than 1 m/s were retained for ambient noise analysis.

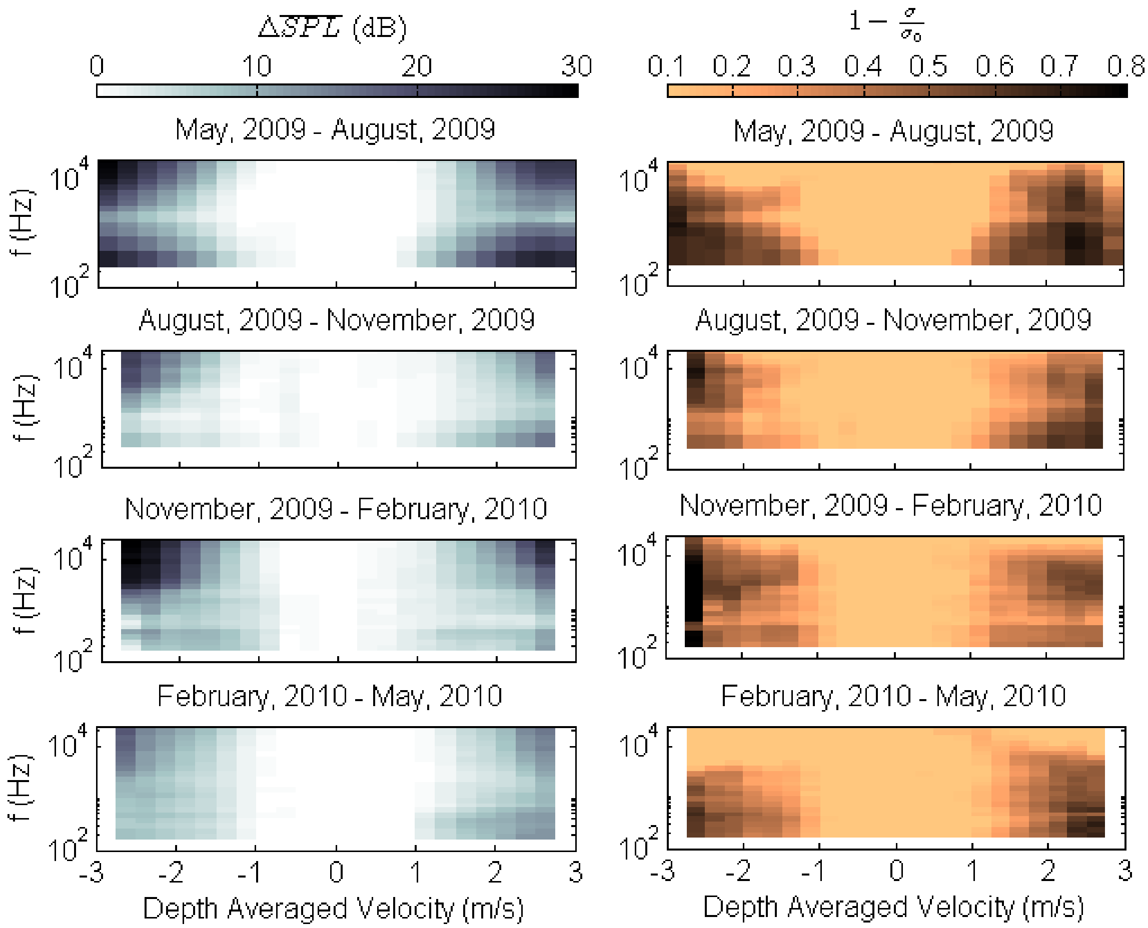

Figure 3.6: Mode shift and normalized σ shift.

Table 3.1: Total number of acoustic samples and the number uncontaminated by flow noise.

Deployment	**Total Recordings**	**Uncontaminated Recordings**	**Percent Uncontaminated**
May, 2009 - Aug., 2009	10847	4567	42.1
Aug., 2009 - Nov., 2009	13951	5495	39.4
Nov., 2009 - Feb., 2010	12272	5989	48.8
Feb., 2010 - May, 2010	10886	4215	38.7
May, 2009 - May, 2010	47957	20266	42.3

Chapter 4

AMBIENT NOISE: RECORDING HYDROPHONE

The four recording hydrophone deployments yield significant amounts of data about ambient noise at the site. The analysis will focus first on characterizing typical ambient noise conditions using mean sound pressure levels, permanent noise levels, and cumulative probability distribution functions. In depth analysis specific to different noise sources is included in Chapter 6.

Different noise sources have unique acoustic signatures. The spectra in Figure 4.1, all recorded on January 4, 2010, except the biological noise recorded on January 2, 2010, demonstrate the variability of dominant frequencies and pressure spectral densities in the vicinity of the site due to common sources. The total sound pressure levels (0.02 - 30 kHz) are 138 dB for the ship recording, 127 dB for the ferry recording, 112 dB for the rain recording, and 105 dB for the quiet recording. Before and during the orca vocalization the total SPL is 109 and 116 dB respectively. During the ship recording, a ship is approximately 2 km from the site in the Northbound shipping lane. In the ferry recording the Keystone-Port Townsend ferry is approximately 1.5 km from the site. Notably, pressure spectral densities in the rain recording are low between 200 Hz and 2 kHz but for frequencies associated with the spectral peak of light rainfall ($f >$ 10 kHz), spectral levels exceed those of ferry and ship traffic.

A time series representation of spectra, or spectrogram, is an effective means of demonstrating acoustic variability with time. Each column in the spectrogram represents one spectrum where the x-axis is the time, the y-axis is the frequency, and the magnitude of the PSD is represented by a colormap. The spectrogram for October 26, 2009 (Figure 4.2) shows typical ambient noise patterns at the site. For continuity, the periods of psuedosound, approximately 07:00 to 09:00 and 14:00 to 16:00, are included in the times series although they are not included in the further analysis.

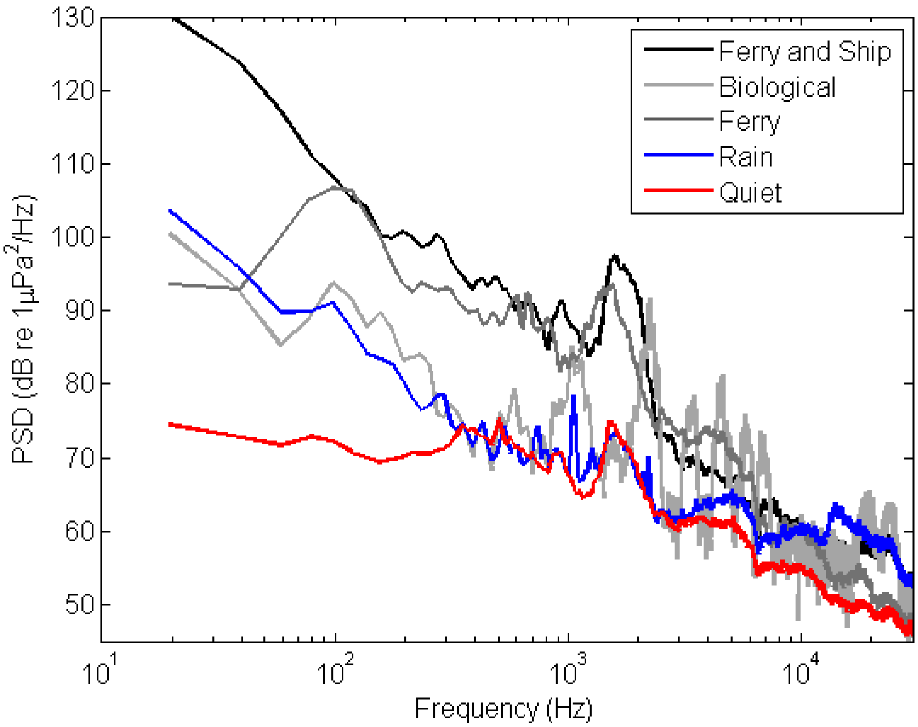

Figure 4.1: Acoustic spectra for under different conditions

The time series representation of the October 26, 2009 data presented in one-third octave band sound pressure levels illustrates the same patterns seen in the spectrogram (Figure 4.3). Although pressure spectral densities are generally lower at higher frequencies, one-third octave bands are integrated over frequency bands that are proportional to the center frequency and therefore sound pressure levels are comparable in magnitude. At the site, the one-third octave band SPLs at the low frequencies are typically the highest in the absence of a noise source at high frequencies. For example, during the period of rain between 02:00 and 07:00 the one-third frequency bands centered in frequencies above 10 kHz are elevated and in some cases exceed SPLs at lower frequencies. When ship and ferry traffic is present there are broadband SPL increases consistent with the mechanical noise, vibrations, and cavitation produced by ship traffic. Well pronounced examples of broadband increases associated with ship traffic occur at 05:00, 13:30, and 23:30. Regular ferry traffic in Admiralty Inlet affects acoustic spectra daily between 06:30 to 21:45 based on the distance from the ferry to the site. The broadband impact of pseudosound is present between 07:00 to 09:00 and 14:00 to 16:00 although the impact is limited due to relatively weak neap tide currents with maximum depth averaged velocities of 1.8 m/s.

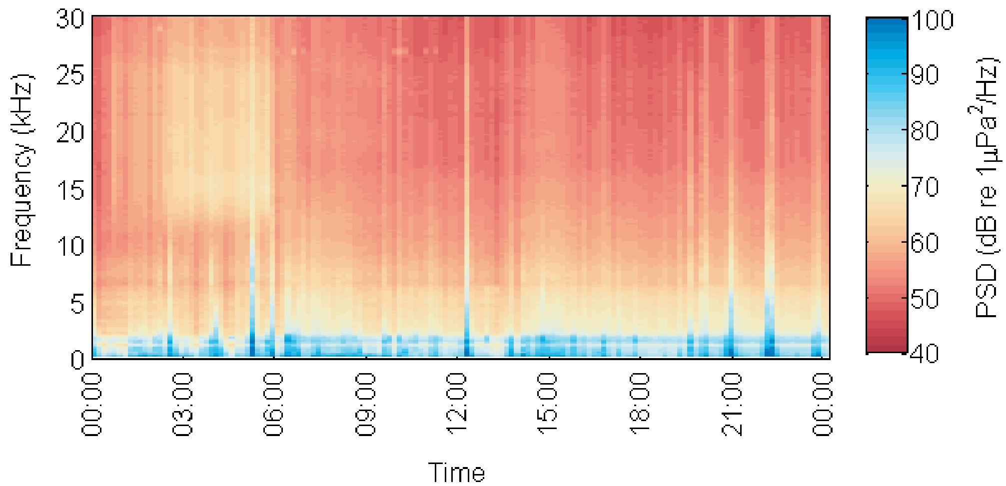

Figure 4.2: Spectrogram for October 26, 2009

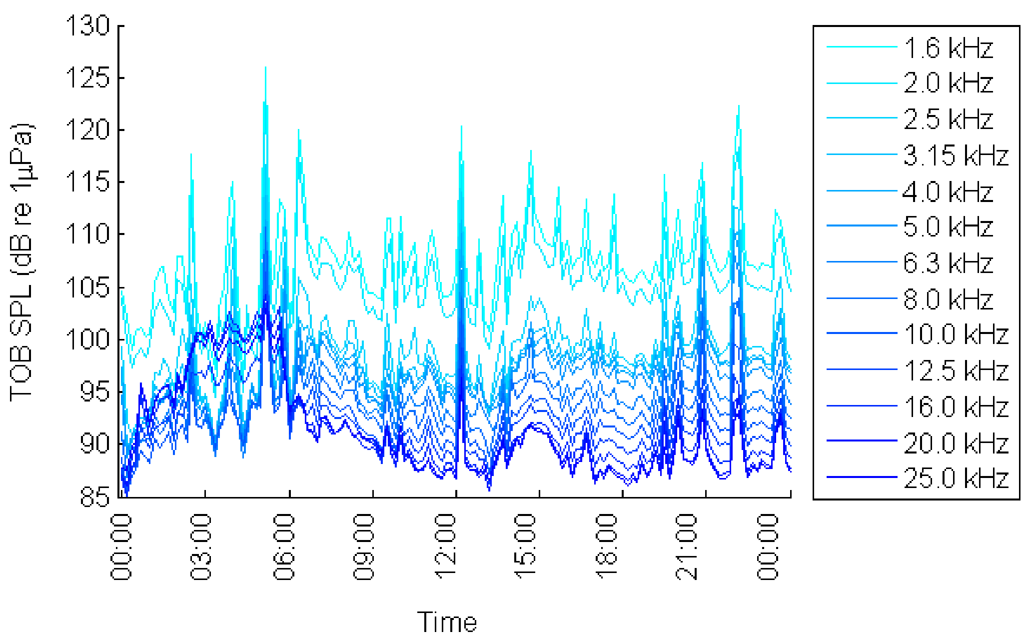

Figure 4.3: One-third octave band sound pressure level time series for October 26, 2009.

On November 5, 2009 normal ferry traffic in Admiralty Inlet was suspended. On November 6, 2009 ferry traffic resumed. Spectrograms and one-third octave band SPLs for the two days are shown in Figures 4.4 and 4.5 respectively. In the spectrogram for November 5, broadband increases pressure spectral density lasting one sample occur throughout the day and are associated with ship traffic in the area. Similar broadband increases occur on November 6, but the increases stand out less due to the regular elevated pressure spectral densities due to ferry traffic. In the early morning and and late evening strong tidal currents result in pseudosound measurements. The one-third octave band SPL time series demonstrate clearly the impact of ferry noise at the site. On November 5, TOB SPLs are relatively constant throughout the day in the absence of ship traffic. On November 6, the TOB SPLs fluctuate substantially more as the ferry transits the Admiralty Inlet.

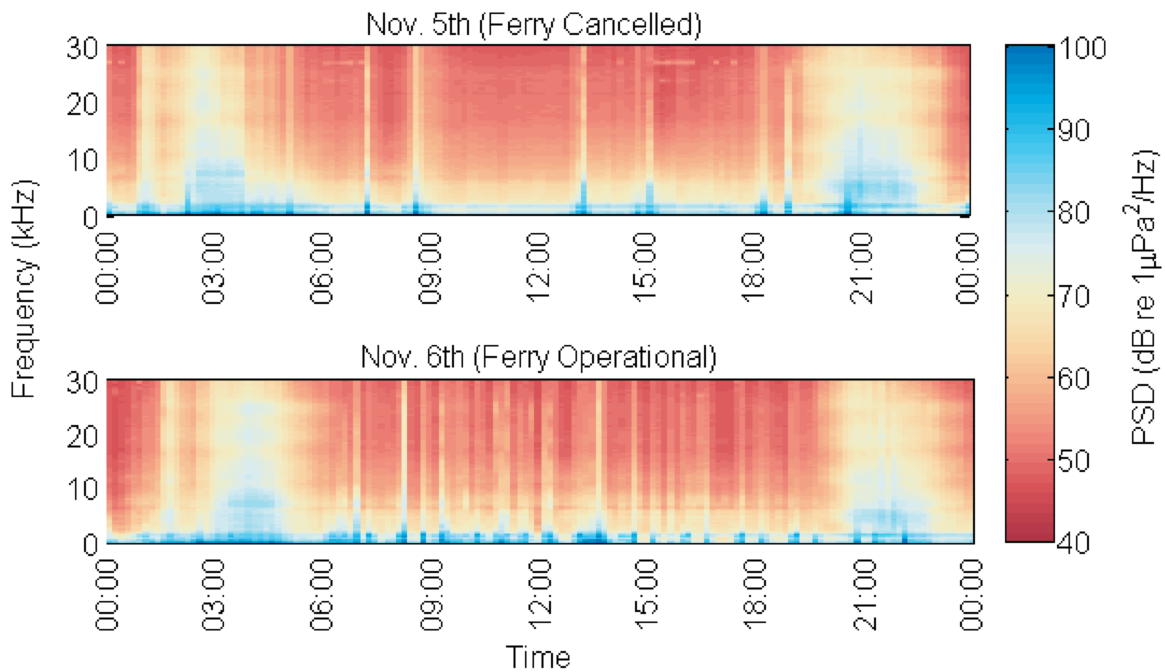

Figure 4.4: Spectrograms for November 5, 2009 and November 6, 2009. Local ferry traffic was canceled due to mechanical problems on November 5 but operating on November 6.

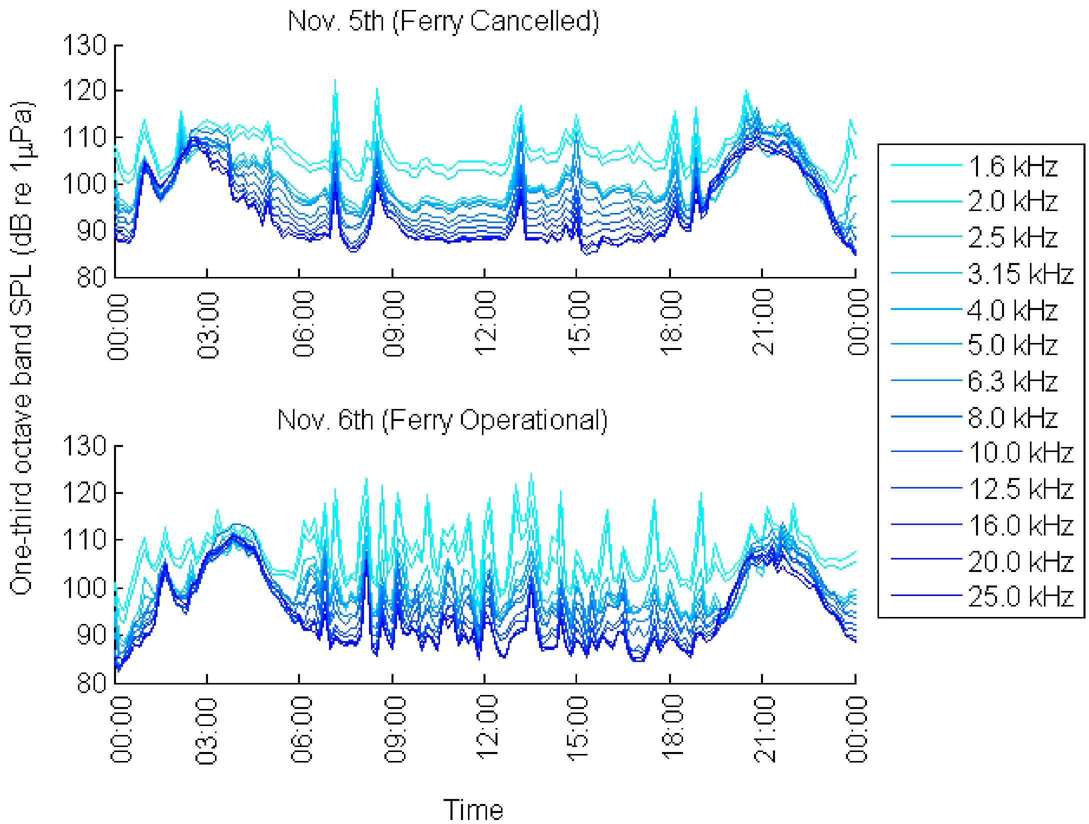

Figure 4.5: November 5, 2009 and November 6, 2009 one-third octave band SPL time series.

The total sound pressure levels throughout each deployment are used to construct a cumulative probability distribution function (CPDF). The CPDF (Figure 4.6) quantifies the percentage of the time that the SPL at the site is equal to or lower than a chosen SPL. The probability density functions for each deployment are Gaussian. The mean total SPLs for the deployments in chronological order are 118, 118, 116, and 117 dB and the standard deviations are 7, 8, 8, and 7 dB respectively. Minimum, maximum, mean total SPLs for all deployments are included in Table 4.1. Nighttime and daytime total SPLs also follow a Gaussian distribution with means 115 and 118 dB and standard deviations of 7 and 8 dB respectively. In the analysis, nighttime hours are defined as 22:00 to 06:00, corresponding closely to the schedule of the ferry. The daytime versus nighttime CPDFs for all deployments are included in Figure 4.7. For total SPLs below 130 dB the percentage of time that a given SPL is exceeded at night is less than for daytime measurements - a difference that is most obvious around mean total sound pressure levels where daytime CPDF is 20 percent lower than the nighttime CPDF.

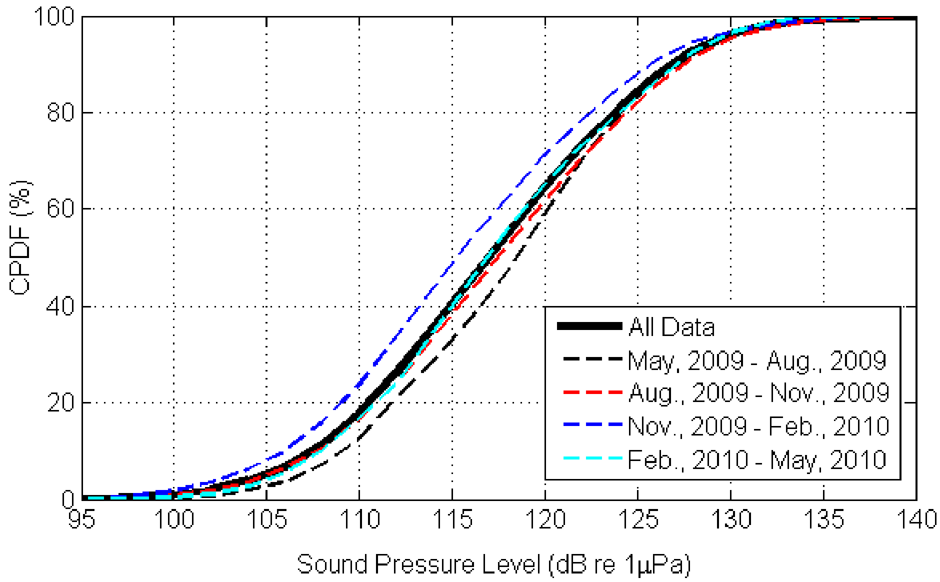

Figure 4.6: Total SPL CPDF (0.156 - 30 kHz) for all deployments.

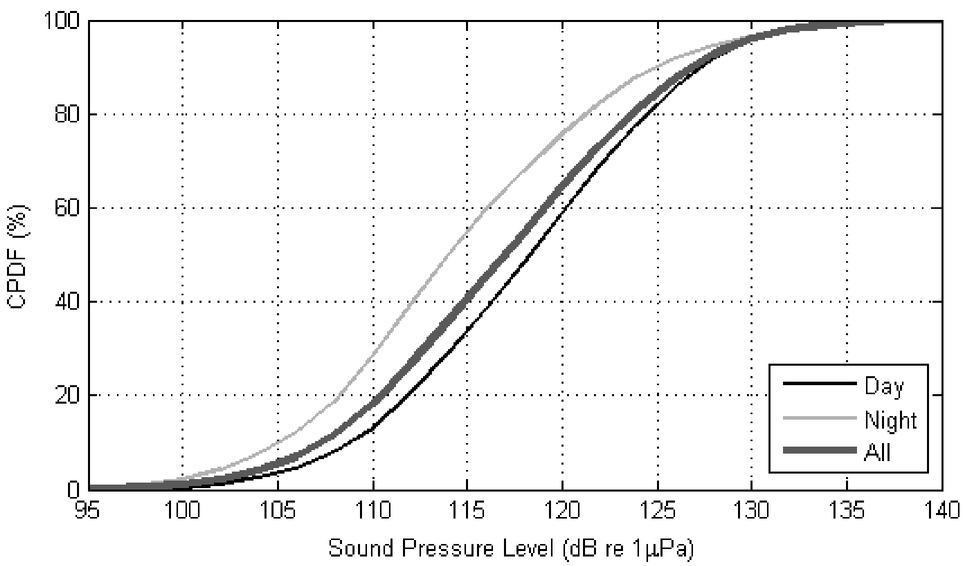

Figure 4.7: Total SPL CPDF (0.156 - 30 kHz) comparing night, day, and all recordings for all deployments.

Table 4.1: Minimum, maximum, and mean total sound pressure levels for each deployment.

Deployment	Total SPL (0.156 - 30 kHz)		
	Minimum	Mean	Maximum
May, 2009 - August, 2009	96	118	140
August, 2009 - November, 2009	97	118	144
November, 2009 - February, 2010	94	116	142
February, 2010 - May, 2010	95	117	141

4.1 Permanent Noise

Qualitatively, permanent noise is defined as the noise present at a site when all identifiable sources have been removed; this is the lowest level of background recurring noise encountered at a site (Dall'Osto, 2009). In contrast, due to the long time series, low duty cycle, and sparse data sets with regard to conditions and potential sources throughout the deployments, permanent noise has been defined as the noise level which is exceeded 99% of the time at the site. This threshold corresponds to a total SPL of 100 dB over the course of the deployments. Using the threshold of 100 dB, ensemble averages of the permanent noise spectra were created for each deployment (Figure 4.8). Permanent noise sound pressure levels in one-third octave band are calculated and presented Table 4.2 and in Figure 4.8. One-third octave bands below 1.25 kHz are not included for the May, 2009 to August, 2009 and August, 2009 to November, 2009 deployments because they cannot be properly resolved using the sampling configuration. Mean permanent noise SPLs for the deployments in chronological order are 98, 99, 98, and 99 dB. The lowest total sound pressure level recorded at the site is 94 dB.

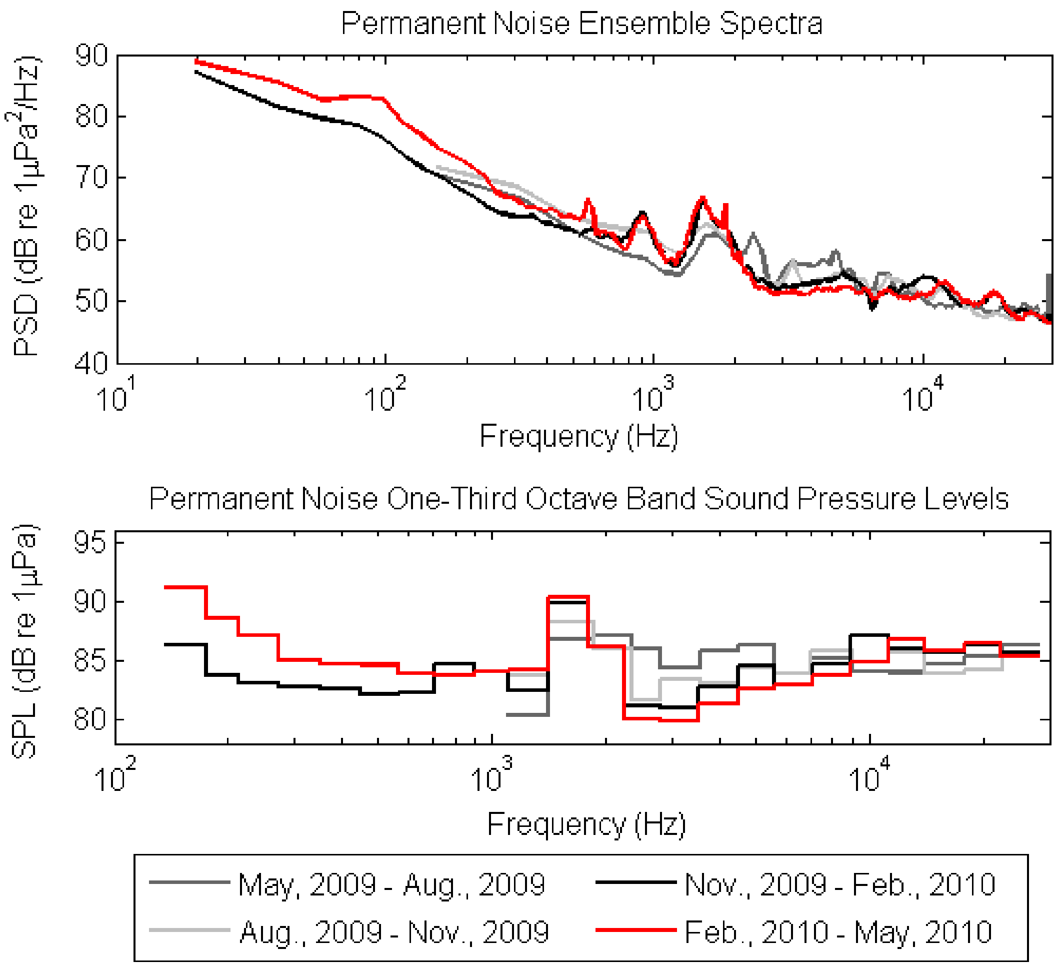

Figure 4.8: Permanent noise spectra.

Table 4.2: One-third octave band permanent noise levels.

f_o (Hz)	**One-third Octave Band SPL (dB re 1 μPa)**			
	May - Aug.	Aug. - Nov.	Nov. - Feb.	May - Feb.
160	-	-	86	91
200	-	-	84	89
250	-	-	83	87
315	-	-	83	85
400	-	-	83	85
500	-	-	82	85
630	-	-	82	84
800	-	-	85	84
1000	-	-	84	84
1250	80	84	82	84
1600	87	88	90	90
2000	87	86	86	86
2500	86	82	81	80
3150	84	83	81	80
4000	86	83	83	81
5000	86	84	84	83
6300	84	84	83	83
8000	85	86	85	84
10000	84	85	87	85
12500	84	86	86	87
16000	85	84	87	86
20000	85	84	86	86
25000	86	85	86	85

Chapter 5

AMBIENT NOISE: CABLED HYDROPHONE

The primary purpose of the cabled hydrophone is to measure sound on multiple spatial scales throughout the project area. During each research cruise, a series of acoustic recordings were performed at distances of 250 m, 500 m, 1000 m, 1500 m, 2000 m, and 2500 m. Each set of recordings includes acoustic measurements at three different depths in the water column: 3 m, 25 m and 50 m beneath the surface. The research vessel is free drifting throughout the measurements so tidal current are required to push the ship between recordings. Spatial acoustic recordings are planned in advance of the cruises and the measurements were taken at the planned times irrespective of transient sources near the site. Acoustic surveys are presented from 41 different geographic positions. Additional recordings have been excluded from the analysis due to potential contamination of the recordings by the strumming of the hydrophone cable, a problem common in measurements taken in high flow environments.

The processing algorithm for cabled hydrophone data is comparable to the recording hydrophone processing but the presentation of sound pressure levels focuses on spatial variability, not temporal. Figure 5.1 includes spectra that represent different acoustic conditions near the site. Notes about anthropogenic noise sources present during the recordings are taken to aid in interpretation of the spectra.

During the samples from August 3, 2009 at 18:15 (Recording 10) a sea plane and the Keystone-Port Townsend ferry were near the site. Apart from natural variability due to reflection at the surface or natural propagation of sound, the differences between the spectra can be explained by the proximity of the recordings to the ferry and the elapsed time between the measurements at different depths. During the sample from August 3, 2009 at 17:45 (Recording 7) there were no ships appearing on the AIS (Automatic Identification System) between Port Angeles and Seattle. Furthermore, the local ferry was in the terminal at

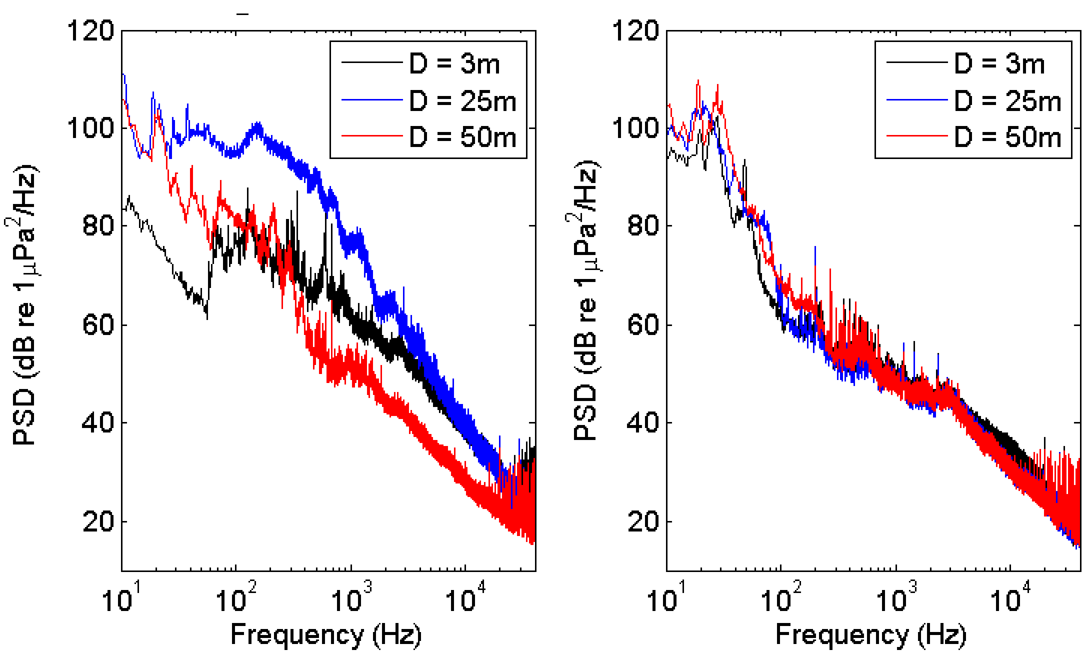

Figure 5.1: Sample spectra from cabled hydrophone recordings. Recording 10 (left) was taken 2000m from the tripod deployment site on 8/4/2009. Recording 7 (right) was taken 1000m from the target on 8/3/2009.

Keystone. The only anthropogenic noise source that was visually identified above water was a sea plane that passed overhead during the recording. Using data from 41 different mobile hydrophone samples during the April, August, and November research cruises, minimum one-third octave band and total sound pressure levels are calculated for each depth in the water column (Table 5.1).

The total SPL is plotted versus the geographical coordinates of each recording in Figures 5.2 and 5.3. For each geographic location, the recordings at different depths are plotted from the Southeast to Northwest with the shallowest sample in the Southeast. Figure 5.3 shows the total SPL for 0.02 to 40 kHz and Figure 5.2 show the total SPL for 0.156 to 30 kHz to provide a direct comparison with stationary hydrophone data. The large green dot show the coordinates of the deployments including the November, 2009 - February, 2010 deployment. The rings show the concentric circles spaced around the site of the November, 2009 to February, 2010 deployment in intervals of 500 m. The results suggest that there is no particular spatial pattern and that SPLs near the site are driven primarily by anthropogenic sources and weather conditions.

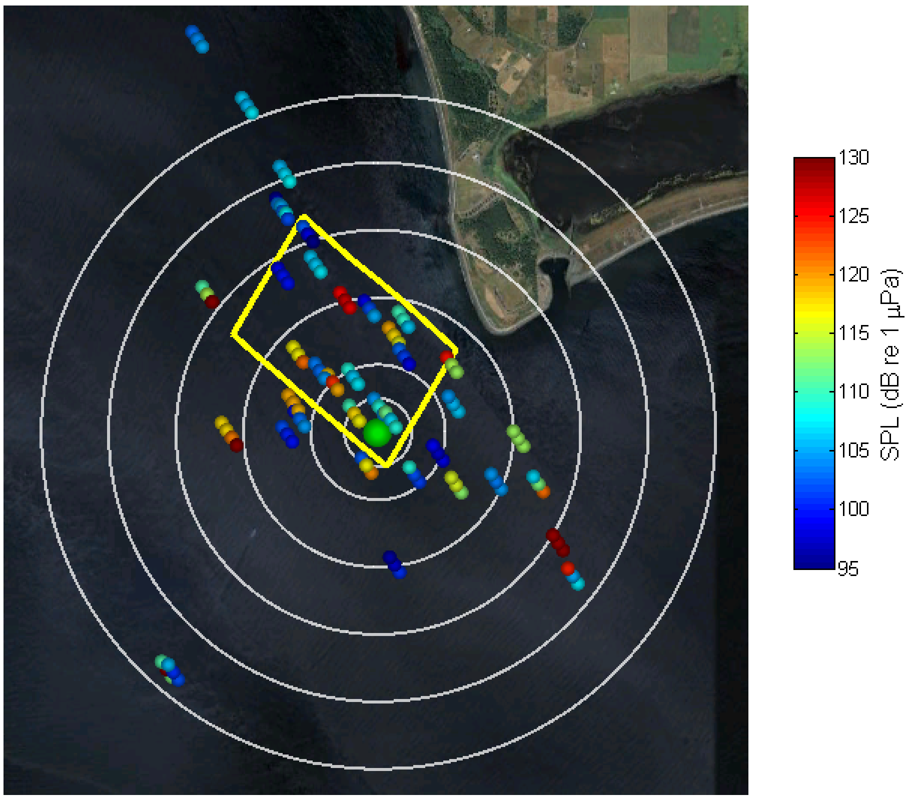

Figure 5.2: Cabled hydrophone total sound pressure levels ((0.16 - 30 kHz).

The cabled hydrophone recordings are conducted near slack water to reduce the potential for cable strum. As a results, depth averaged tidal currents during the recordings are relatively low and do not reflect any potential variations due to tidal currents at the site. Recorded transient sources near the site included container ships, coast guard vessels, tug boats, ferries, sea planes, and recreational boat traffic. Recordings are also conducted with no visually confirmed anthropogenic noise sources in the area. All recordings in April and May were performed with calm seas with no rain. In November seven recordings were taken during a period with substantial breaking waves and during a period with calm seas. No cabled hydrophone recordings include precipitation.

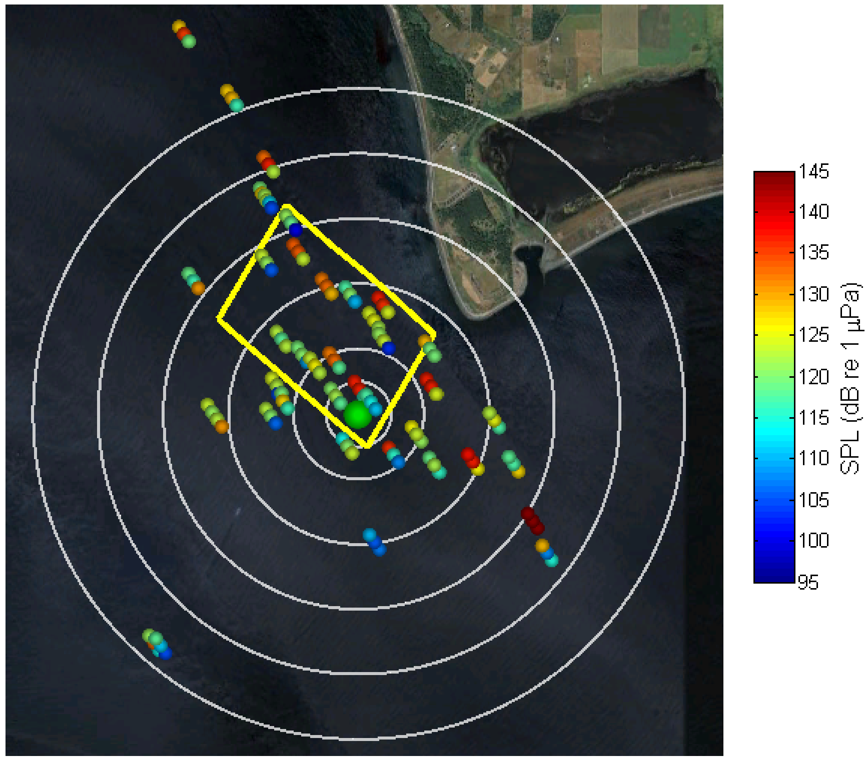

Figure 5.3: Cabled hydrophone total sound pressure levels (0.02 - 30 kHz).

Sound pressure levels are also presented in one-third octave bands. Due to the high frequency resolution, approximately 1.5 Hz, one-third octave bands are resolvable down to a center frequency of 25 Hz. To determine the lowest levels recorded near the site the minimum sound pressure level in each frequency band is determined irrespective of the recording in which it was taken. This method is repeated for each depth in the water column. The lowest total sound pressure level (0.02 - 30 kHz) is also reported for each depth. The results are shown in Table 5.1.

Total sound pressure levels (0.156 - 30 kHz) from the cabled hydrophone range from 95 dB to 133 dB, a range comparable to that of the recording hydrophone data. Total sound pressure levels from 0.02 to 30 kHz range from 99 dB to 139 dB. One sample recorded a total sound pressure level (0.02 - 30 kHz) of 147 dB. However, this number is suspect. While two ships are approximately two kilometers from the site substantial cable strumming is also noted in the acoustics log.

Table 5.1: Minimum one-third octave band sound pressure levels recorded with the cabled hydrophone.

f_o (Hz)	**TOB SPL (dB re 1μPa)**			f_o (Hz)	**TOB SPL (dB re 1μPa)**		
	3m	25m	50m		3m	25m	50m
25	85	98	97	1000	78	83	82
31.5	84	93	93	1250	82	85	84
40	80	90	86	1600	82	81	81
50	78	86	89	2000	81	79	80
63	83	89	89	2500	75	78	77
80	84	87	89	3150	75	77	76
100	85	89	86	4000	74	77	77
125	86	85	84	5000	76	76	77
160	87	87	87	6300	76	74	76
200	83	88	84	8000	75	73	73
250	79	85	84	10000	72	72	71
315	78	84	83	12500	71	71	70
400	80	82	80	16000	71	71	70
500	82	82	82	20000	70	70	70
630	79	83	82	25000	71	70	70
800	80	84	83	20 - 30000	99	105	104

Chapter 6

SOURCES

Wind, rain, anthropogenic sources, and biological sources contribute to total noise levels at the site. With the exception of biological noise, most sources originate near the air-sea interface. Data obtained from various sources and hydrophone data are used to document the influence and extent of ship noise, the impacts of precipitation, and identify transient biological noise at the site.

6.1 Ship Noise

Ship noise is the dominant noise source at the site. A rigorous analysis of typical source levels of ships passing through Admiralty Inlet is not currently possible given the available storage capacity of the Loggerhead DSG system. Shipping vessels passing rapidly through Admiralty Inlet only produce a strong signal for during one or two recordings because of the 1% duty cycle and 10 minute sample spacing.

Washington State Ferries, also equipped with AIS, can be used as a proxy to determine the impact of all shipping traffic at the site. Strong tidal currents, changing weather conditions, variability in driving, and varying physical conditions governing sound propagation (e.g. sound speed profiles or bathymetry) invalidate the assumptions that the ferry has a constant source level and that different frequency noises will propagate from the source to the site equally from different geographic locations. Nevertheless, six weeks of ferry traffic and acoustics data is used to estimate the ferry source level.

Using data from December 13, 2009 to January 15, 2010 and January 24, 2010 to January 31, 2010 a plot of total sound pressure levels with the ferry in transit was created (Figure 6.1). A continuous one month set of data was not available due to a storm which interrupted power to the AIS receiver installed at the lighthouse at Ft. Casey State Park. To isolate the ferry as the primary source of anthropogenic noise at the site an algorithm

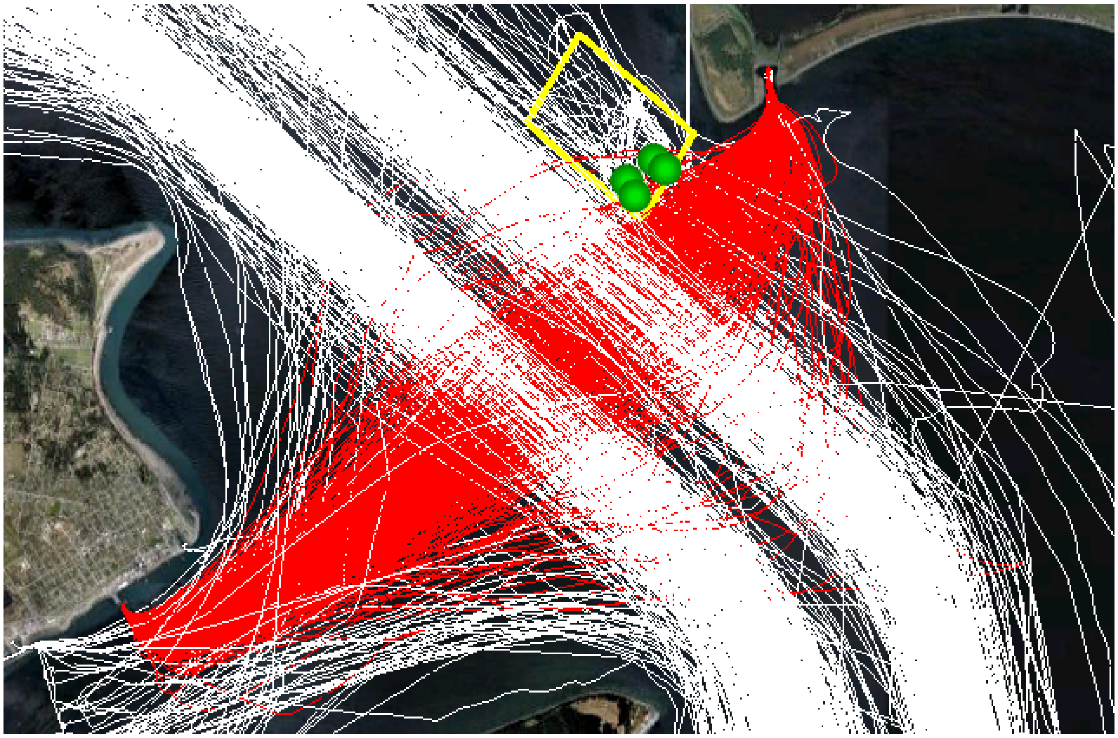

Figure 6.1: All ship and ferry traffic obtained by AIS system in Admiralty Inlet in February, 2010.

removes any recordings in which any ship besides the ferry is within 9 km (approximately 5 nautical miles). The ferry terminal in Port Townsend is approximately 6.4 km from the site meaning that if another ship is approaching Admiralty Inlet it is at least 2.5 km further from the site than the ferry. Recordings in which the ferry is approaching a terminal and samples contaminated by flow-noise are also removed.

Over the six weeks analyzed there were 368 acoustic samples that met the aforementioned criteria. The location of the ferry during recordings is well distributed spatially over the six weeks even though there some areas have a larger number of samples due to the constant ferry and acoustic recording schedules. With all other sources removed, the total SPL recorded decreases as the distance to the ferry increases as shown in Figure 6.1. The pattern is a result of transmission losses from the acoustic source. Outliers may be related to vessel traffic not picked up by the AIS, irregular transits, or some other unidentifiable source.

A commonly used method for estimating source levels at one meter is to take acoustic measurements at a number of distances from a source, plot the total SPL versus the log of the distance, and fit a line to the data. The resulting intercept of the line of fit is the estimated source levels and the slope is a measure of the geometric spreading. The method, while commonly used, assumes a compact source with a constant source level, neglects changes in sound speed, reflection of sound from the substrate, and changes in bathymetry. The assumption that the source level is constant is not reasonable because the acoustic power produced by the ferry is dependent on the mechanical usage of the ferry (e.g. engine throttle). Therefore, variables such as the weather and tidal currents are likely correlated with the acoustic power of the ferry. Without more information on sea state addressing the impacts of weather is not possible. The results from the 368 unique recordings with a confidence interval of 95% suggest a source level of 179 ± 4 dB at 1m.

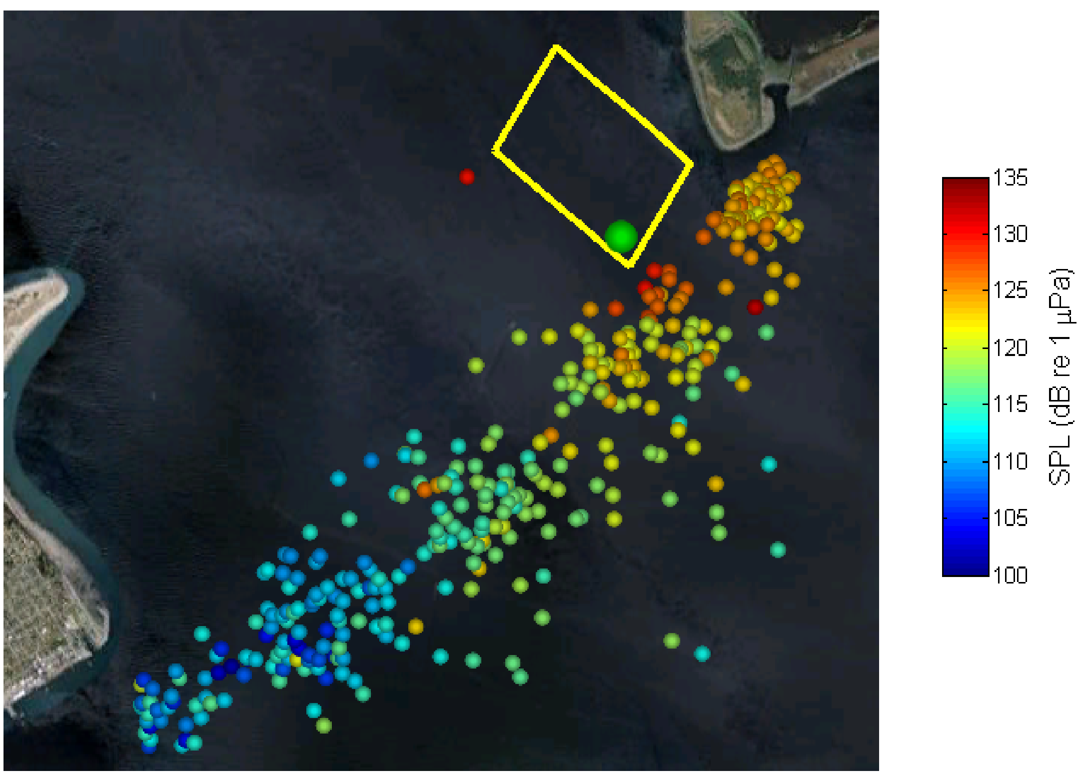

Figure 6.2: SPLs recorded at the site (large green dot) plotted at the location of the ferry when the recording was taken.

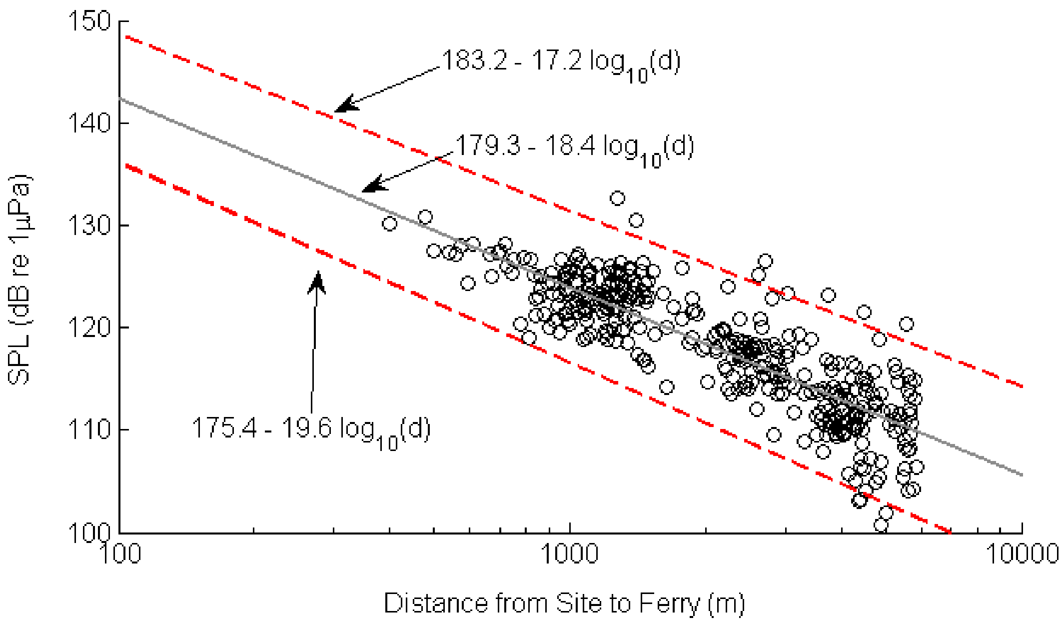

Figure 6.3: Ferry source level and the geometric spreading estimations with 95% confidence intervals.

6.2 Rain

The acoustic signature of light rain is increased spectral levels between 10 and 30 kHz with a wind dependent peak around 15 kHz. Potential periods of rain are identified with a thresholding algorithm that searches for spectra in which pressure spectral densities are 4 dB louder at 15 kHz than at 9 kHz. The algorithm is adapted from a semi-empirical model developed for predicting underwater sound levels from precipitation published in Ma et al. (2005). The thresholding algorithm works in the absence of biological noise because the acoustic spectra associated with wind and ship traffic are red, meaning that pressure spectral densities decrease with increasing frequency. Light rain produces a spectral peak that stands out from an otherwise red spectrum allowing the basic algorithm to recognize such deviations. Daily and hourly precipitation data from the Washington State University Agricultural Weather Network station on Whidbey Island is compared with algorithm results.

During the May, 2009 through May, 2010 deployments a total of 109 days of precipitation were recorded at the station on Whidbey Island. Table 6.1 includes the number of days reported with different precipitation rates and the results from the detection algorithm. For days with precipitation rates greater than 2 mm/hr the detection rates are 71%. For days with maximum precipitation rates less than 0.5 mm/hr detection rates are 30%. This can be explained by the fact that low precipitation rates (< 2 mm/hr) are associated with small droplets that may not entrain air and therefore may not be detectable above ambient noise. Eight additonal days contain acoustic signatures consistent with rainfall when it is not reported at the Whidbey Island station. It is likely that periods of rainfall are masked by pseudosound but this cannot be confirmed without precipitation data specific to the deployment site.

Table 6.1: Reported and detected precipitation.

Max. Precip. Rate	**Days Reported**	**Days Detected**	**Percent Detected**
> 2 mm/hr	21	15	71
> 1 mm/hr	47	32	68
> 0.5 mm/hr	74	46	62
< 0.5 mm/hr	33	10	30
> 0 mm/hr	109	55	50
None	-	8	-

For each deployment ensemble averages of the precipitation events detected by the algorithm are show in Figure 6.4. It is possible that the the broader peak in the November, 2009 to February, 2010 deployment can be explained by the broadening of the spectral peak during moderate wind events but this cannot be confirmed with the available data set.

A comparison of sound pressure levels in one-third octave bands for permanent noise conditions and average rainfall event is included in Table 6.2. Sound pressure levels in one-third octave bands centered at 10 kHz to 25 kHz have average rainfall values that

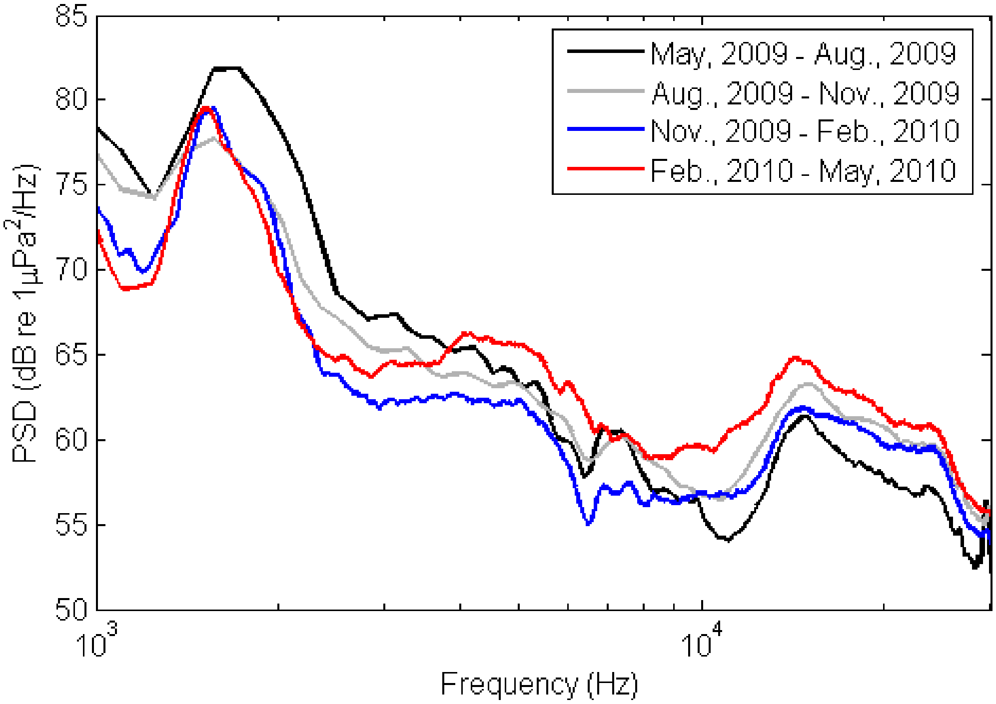

Figure 6.4: Average spectra for precipitation events detected by the rainfall algorithm during the all four deployments.

exceed permanent noise levels in their respective frequency bands by at least 7 dB. The largest increases occur in the one-third octave band that contains the spectral peak for light rainfall (f_o = 16 kHz), sound pressure levels are between 12 and 16 dB above permanent noise levels.

6.3 Biological Noise

Common cetacean and pinniped species in Puget Sound include but are not limited to killer whales, harbor porpoises, Stellar sea lions and harbor seals. While harbor porpoises are quite common near the site their echolocation clicks are well above the range of the recording hydrophone. Information on SRKW transits and detected vocalizations in Admiralty Inlet are used to determine the best times to search for suspect biological noise. Public information available from the Orca Network, the Port Townsend Marine Science Center hydrophone, and correspondence with Beam Reach Marine Science and Sustainability School

Table 6.2: Average one-third octave band SPLs for detected precipitation events where PN refers to the permanent noise level.

	Deployment							
f_o **(Hz)**	**May - Aug.**		**Aug. - Nov.**		**Nov. - Feb.**		**Feb. - May**	
	Rain	PN	Rain	PN	Rain	PN	Rain	PN
10000	88	84	93	85	91	85	85	93
12500	92	84	97	86	95	87	87	97
16000	96	85	101	84	98	86	86	99
20000	95	85	100	84	97	86	86	98
25000	94	86	99	85	96	86	82	97

provided times and dates of recorded killer whale vocalizations and transits in Admiralty Inlet. Acoustic data within one hour of an sighting, human reported vocalization detection or an auto-detection at the Port Townsend Marine Science Center hydrophone are reviewed. Given that automated vocalization detection would require significant algorithm development and is not the primary goal of this study, a simple method of reviewing spectrograms and listening to audio files is used to detect possible biological noise.

One motivation for changing to a short but continuous sampling regime is to facilitate identification of potential vocalizations. As a result, all suspected vocalizations are from the November, 2009 - February, 2010 deployment; the season which also has the largest number of historical transits by SRKWs. Spectrograms are created using raw pressure spectral densities with a bandwidth of 19.53 Hz. Each spectrum is created with 4096 raw data points over a period of 0.0512 seconds but a 50% overlap so each plotted spectrum steps forward 0.0256 seconds in the spectrogram. Ambient sound pressure levels are calculated by taking ensemble averages of spectra outside of the interval of vocalizations and integrating over the frequency bands. Table 6.3 includes the dates, times and total sound pressure levels for the cases of suspected biological noise.

With the exception of the biological noise recorded on 11/23/09 and 12/4/09, ambient

Table 6.3: Suspect biological noise dates, times and ambient SPLs.

Date	**Time**	**Ambient SPL** (0.156-30 kHz)	**Ambient SPL** (0.02-30 kHz)
11/23/09	02:10	119	122
11/25/09	17:50	114	114
12/4/09	20:20	116	117
12/4/09	20:30	121	122
12/10/09	18:50	109	116
12/10/09	19:00	107	112
12/22/09	15:10	107	110
12/22/09	15:20	107	121
12/22/09	15:50	106	112
1/2/10	14:20	107	117
1/2/10	14:50	109	115
1/4/10	07:40	116	125
2/4/10	16:50	102	105

noise levels are below mean ambient noise levels at the site. The resulting spectrograms reveal different vocalization types found in frequency bands. The final resolution of the vocalization is dependent on the signal to noise ratio and therefore the ambient noise levels and the proximity of the source. As a result, specific spectrograms yield a much clearer image of the calls than others.

Figure 6.5 is a spectrogram of the entire sample recorded on 1/2/10 at 14:20. The spectrogram shows a well defined upsweeping vocalization lasting approximately one second with a frequency range of 2 kHz to 10 kHz. Two distinct two second long vocalizations with frequencies between 1.5 and 5.25 kHz were recorded on 12/10/09 at 18:50 (Figure 6.6).

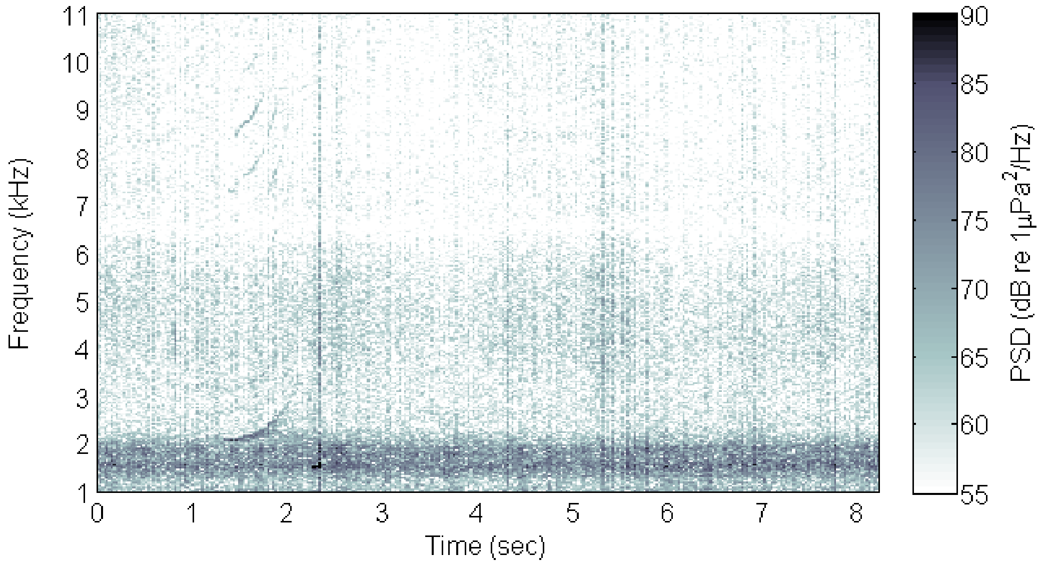

Figure 6.5: Vocalization recorded on 1/2/10 at 14:20.

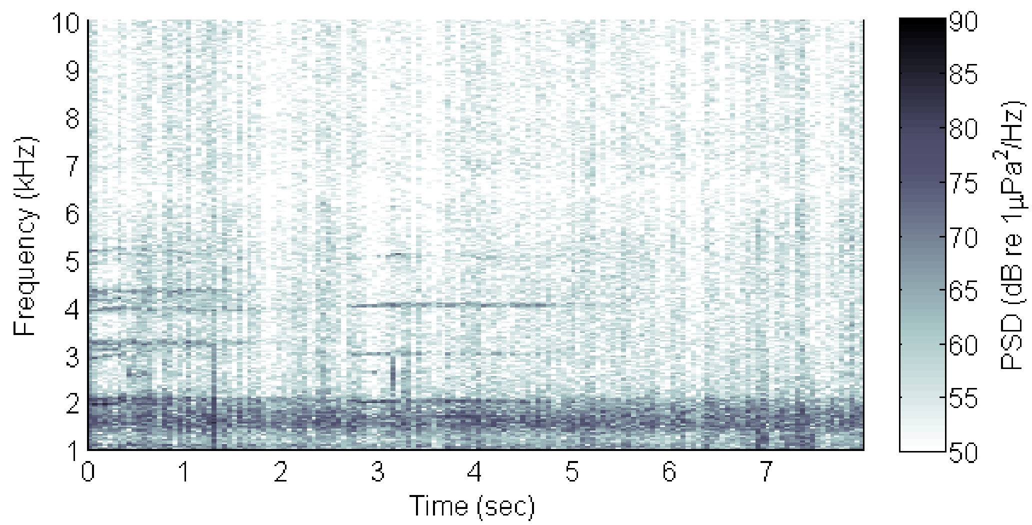

Figure 6.6: Vocalization recorded on 12/10/09 at 18:50.

The acoustic recording taken on 12/22/09 at 15:50 (Figure 6.7) includes three distinct vocalizations. The first, covering frequencies from 1.5 to 2.25 kHz ended just after the recording began. Two seconds into the recording a downsweep lasting approximately 0.6 seconds with frequencies between 1 and 2 kHz occurs. The final vocalization, beginning around 5.5 seconds, lasts about 1 second although the frequency range (approximately 1.25 to 2.25 kHz) fall within the spectral peak of ambient noise and is hard to resolve.

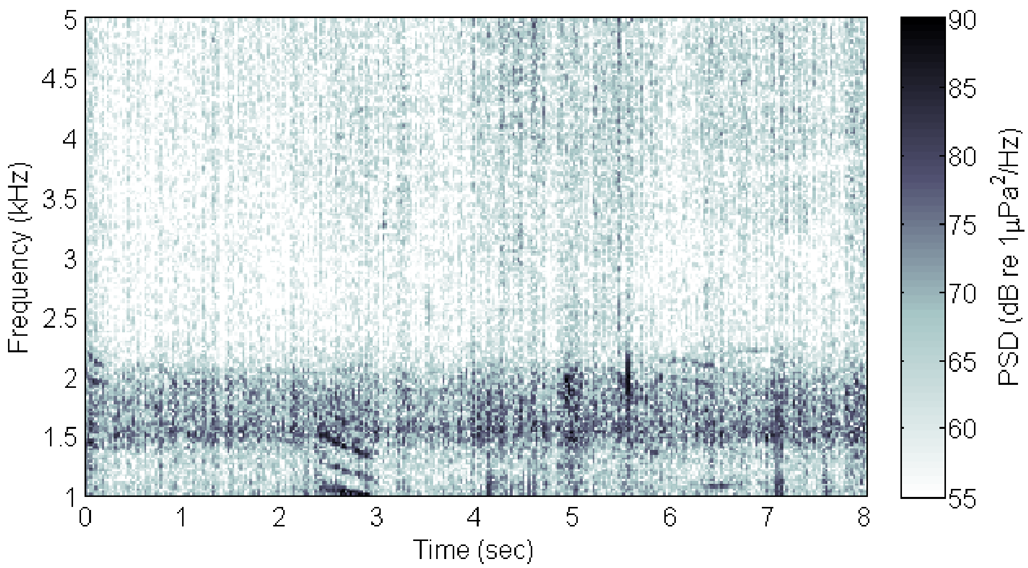

Figure 6.7: Vocalization recorded on 12/22/09 at 15:50.

Some of the other suspected biological noise incidents include a sample on 12/22/09 at 15:10 including multiple distinct vocalizations, a recording from 12/22/09 at 15:20 with a broadband click sound and a strong signal of an upsweeping vocalization from 1/2/10 at 14:50 that is cut off because the recording ends just as the call begins.

Chapter 7

CONCLUSION

Acoustics data collected over a one year period with 1% duty cycle demonstrate that the underwater noise conditions in Admiralty Inlet are affected by a number of sources, the most dominate of which is anthropogenic noise. A staggered sampling configuration allows for sampling over longer periods of time and the results are comarable to continuous sampling for shorter periods of time. Continuous sampling is an effective method of recording and idenitying transient noise sources like cetacean vocalizations. Although sea planes, industrial activity in Port Townsend, and small recreational boats may affect recorded sound pressure levels, the greatest contributors to the noise budget are the Keystone-Port Townsend ferry and commercial ship traffic. Everyday the Port Townsend-Keystone ferry is in transit in the area for approximately 12 hours. Additional ships, such as the Victoria Clipper, a number of shipping vessels, and tug boats with barges, pass the site on a daily basis. Rain, wind, and biological sources also impact recorded ambient noise levels at the site but can be difficult to identify without the development of algorithms or additional information. The integration of data about weather and ship traffic from other sources is an important component of understanding contributions to ambient noise in the area and understanding how tidal energy development may affect important marine species that inhabit or transit the area.

Sites suitable for tidal energy are inherently energetic sites which means that acoustic measurements are susceptible to pseudosound, non-propagating pressure fluctuations that are measured by a pressure sensitive hydrophone by are not propagating sound. Care must be taken to ensure that measurements of pseudosound are not included in descriptions of background noise at a proposed site.

Permanent noise at the site is 98 dB re 1 μPa and the mean total sound pressure level is 117 dB re 1 μPa. Total sound pressure levels drop below 100 dB re 1 μPa approximately

1% of the time and exceed 130 dB re 1 μPa approximately 4% of the time. Mean daytime broadband sound pressure levels are 3 dB re 1 μPa louder than nighttime levels due to ferry traffic. Light rainfall events impact acoustic spectra between 10 and 30 kHz have been documented and compared with weather data from Whidbey Island. In the absense of ship traffic very close to the site or pseudosound a basic thesholding algorithms are able to detect precipitation. During precipitation events one-third octave band sound pressure levels exceed permanent noise levels by at least 7 dB re 1 μPa with the largest increases, greater than 12 dB re 1 μPa, in the one-third octave band centered at 16 kHz.

With careful analysis, cases of biological noise are identified and the presence of marine mammals in the area has been confirmed by other parties. Of the 13 recordings with suspected biological noise during the November, 2009 to February, 2010 deployment, only two are identified when the total ambient SPL (0.156 - 30 kHz) is above the mean total SPL of 116 dB re 1 μPa for the deployment. The positive identification numerous SRKW vocalizations demonstrates that the bottom mounted hydrophone can effectively capture transient biological noise events. An increased duty cycle and techniques for mitigating pseudosound would likely lead to further positive identification of marine mammal vocalizations in the frequency ranges under consideration.

Analysis of the cabled hydrophone data shows sound pressure levels consistent with those measured by the recording hydrophone and no dependence on depth or distance from the site. Sound pressure levels from cabled hydrophone data reflect acoustic variability as a result of weather and anthropogenic sources in Admiralty Inlet. Significant spatial differences in the immediate vicinity of the site are unlikely given that the most common acoustic sources ensonify the entire area under consideration.

Chapter 8

FUTURE WORK

A method was developed so that only acoustic samples uncontaminated by pseudosound were considered in the ambient noise analysis. During periods of elevated velocities, cobbles shifting on the sea floor are a source of true propagating noise that has not been analyzed due to the presence of pseudosound. Coherence calculations using two hydrophones can be used to identify periods of flow-noise and to explain to what extent moving cobbles on the floor are responsible for increases sound pressure levels during periods of strong currents. In order to analyze the contribution a method should be developed to mitigate the effects of pseudosound. One possibility is to deploy a Lagrangian drifter that will follow the currents at the surface while acquiring data.

In order for a cabled hydrophone deployed near the site of a tidal turbine to effectively measure sound during high currents, a methodology needs to be developed for properly measuring propagating sound in highly energetic and turbulent environments from a stationary platform. Without precautions, any acoustic measurement system deployed at the site in order to measure ambient noise conditions would be seriously affected by pseudosound at the times during which it is most important to take measurements.

Post processing of real-time AIS system can be used to associate ship traffic with sound pressure levels at the site. AIS data strings include more information that can be used for additional statistical analysis at the site. Using data collected over a longer period of time individual ship identification numbers can be used to calculate hourly, daily, monthly, and seasonal variations in ship traffic. Average ship velocities and transit times in Admiralty Inlet can be used to calculate how often ships are near the source. Ship length and vessel tonnage statistics, combined with ship velocities, can be used predict ship source levels based on available source level statistics for shipping traffic. Lastly, ship draft data can be used to determine the overhead clearance required for a turbine array.

Simulations of a turbine noise will be carried out to in order to make measurements of sound propagation from a known source. During the playback period two tripods equipped with hydrophones will be deployed on the sea floor near the site, hydrophones will be deployed from the research vessel at various depths, and another hydrophone will be deployed from a Lagrangian drifter. The playbacks will allow further quantification of the impacts of tidal turbines on the underwater ambient noise environment.

BIBLIOGRAPHY

Arveson, P. and D. Vendittis (2000). Radiated noise characteristics of a modern cargo ship. *J. Acoust. Soc. Am. 107 (1)*, 118–129.

Au, W., J. Ford, J. Horne, and K. Allman (2004). Echolocation signals of free-ranging killer whales (*Orcinus orca*) and modeling of foraging chinook salmon (*Oncorhynchus tshawytscha*). *J. Acoust. Soc. Am. 115 (2)*, 901–909.

Bracewell, R. (2000). *The Fourier Transform and Its Applications.* McGraw-Hill Inc.

Dahl, P. (2010, February 2). Discussion with Dr. Peter Dahl of the Applied Physics Laboratory/University of Washington.

Dahl, P., J. Miller, D. Cato, and R. Andrew (2007). Underwater ambient noise. *Acoustics Today 3*, 22–33.

Dall'Osto, D. (2009). A study of the spectral and directional properties of ambient noise in puget sound. Master's thesis, University of Washington.

Deane, G. (2000). Long time-base observations of surf noise. *J. Acoust. Soc. Amer. 107 (2)*, 758–770.

Deeke, V., J. Ford, and P. Slater (2005). The vocal behaviour of mammal-eating killer whales: communicating with costly calls. *Animal Behaviour 69*, 395–405.

Emery, W. and R. Thomson (1997). *Data Analysis Methods in Physical Oceanography.* Elsevier Science B.V.

Ford, J. (1989). Acoustic behavior of resident killer whales (*Orcinus orca*) off Vancouver Island, British Columbia. *Can. J. Zool. 67*, 727–745.

Ford, J. (1991). Vocal traditions among resident killer whales (*Orcinus orca* in coastal waters of British Columbia. *Can. J. Zool. 69*, 1455–1483.

Gray, L. and D. Greeley (1980). Source level and model for propeller blade rate radiation for world's merchant fleer. *J. Acoust. Soc. Am. 67 (2)*, 516–522.

Hildebrand, J. (2004). Sources of anthropogenic noise in the marine environment. Technical report, Report to the Policy on Sound and Marine Mammals: An International Workshop. U.S. Marine Mammal Commission and Joint Nature Conservation Committee, UK. Longdon, England. http://www.mmc.gov/sound/internationalwrkshp/pdf/hildebrand.pdf.

Hildebrand, J. A. (2005). *Impacts of Anthropogenic Sound*. The Johns Hopkins University Press, Baltimore, Maryland.

Holt, M. M. (2008). Sound exposure and Southern Resident kill whales (*Orcinus Orca*): A review of current knowledge and data gaps. Technical report, US. Dept. Commer., NOAA Tech. Memo. NMFS-NWFSC-89, pp. 58-60.

Ma, B. B., J. Nystuen, and R. Lien (2005). Prediction of underwater sound levels from rain and wind. *J. Acoust. Soc. Am. 117 (6)*, 3555–3565.

Medwin, H. (2005). *Sounds in the Sea: From Ocean Acoustics to Acoustical Oceanography*. Cambridge, UK: University Press.

Medwin, H., J. Nystuen, P. Jacobus, and L. Ostwalk (1992). The anatomy of underwater rain noise. *J. Acoust. Soc. Am. 92 (3)*, 1613–1616.

Mellen, R. (1952). The thermal-noise limit in the detection of underwater acoustic signals. *J. Acoust. Soc. Amer. 24 (5)*, 478–480.

NMFS (National Marine Fisheries Service) (2006). Endangered and threatenend species designation of critical habitat for Southern Resident killer whales. Technical report, Federal Register [Docket No. 060228057-6283-02, 29 November 2006] 71(229):69054-69070.

NMFS (National Marine Fisheries Service) (2008). Recovery plan for Southern Resident killer whales (*Orcinus orca*). Technical report, National Marine Fisheries Service, Northwest Region, Seattle, Washington. p. 59.

NRC (National Research Council) (2003). *Ocean Noise and Marine Mammals.* Washington, DC: National Academies Press.

Nystuen, J. and D. Farmer (1987). The influence of wind on the underwater sound generated by light rain. *J. Acoust. Soc. Am. 82 (1)*, 270–274.

Priestley, M. (1981). *Spectral Analysis and Time Series.* Academic Press.

Richardson, W. J., C. G. Jr., C. Malme, and D. Thomson (1995). *Marine Mammals and Noise.* Academic Press.

Ross, D. (1976). *Mechanics of Undewater Noise.* Pergamon Press Inc.

Scrimger, P. and R. Heirmeyer (1991). Acoustic source-level measurements for a variety of merchant ships. *J. Acoust. Soc. Am. 89 (2)*, 691–699.

Shepard, A. (2009). Marine mammals of the salish sea. Technical report, San Juan Nature Institute.

Strasberg, M. (1979). Nonacoustic noise interference in measurements of infrasonic ambient noise. *J. Acoustic. Soc. Am. 66 (5)*, 1487–1493.

Strasberg, M. (1988). Dimensional analysis of windscreen noise. *J. Acoust. Soc. Am. 83 (2)*, 544–548.

The Whale Museum. "Days/Months the Orcas Have Been Detected in Puget Sound". http://www.whale-museum.org/education/library/whalewatch/pugetsound.html (accessed January 18, 2009).

Urick, R. (1967). *Principles of Underwater Sound for Engineers.* McGraw-Hill Inc.

Wenz, G. (1962). Acoustic ambient noise in the ocean: Spectra and sources. *J. Acoust. Soc. Am. 34*, 1936–1956.

Whitlow, A., A. Popper, and R. Fay (2000). *Hearing by Whales and Dolphins*. New York, USA: Springer-Verlag.

Wille, P. and D. Geyer (1984). Measurements on the origin of the wind-dependent ambient noise variability in shallow water. *J. Acoust. Soc. Amer. 75 (1)*, 173–185.

Willis, J. and F. Dietz (1965). Effect of tidal currents on 25 cps shallow water ambient noise measurements. *J. Acoust. Soc. Am. 37*, 125–130.